Characterization Techniques and Tabulations for Organic Nonlinear Materials, M. G. Kuzyk and C. W. Dirk, Eds., page 655-692, Marcel Dekker, Inc., 1998

Z-Scan Measurements of Optical Nonlinearities

Eric W. Van Stryland
CREOL
Center for Research and Education in Optics and Lasers
University of Central Florida
Orlando, Florida 32816-2700

and

Mansoor Sheik-Bahae
Department of Physics and Astronomy
University of New Mexico
Albuquerque, New Mexico, 87131

Glossary: Notations and Definitions

α : absorption coefficient

β : two-photon absorption coefficient (ultrafast response)

λ : wavelength

$\Delta\alpha$: change in absorption coefficient

$\Delta\phi = \Delta\phi(z',r,t)$: nonlinearly-induced phase shift

$\Delta\Phi_0$: the on-axis (r=0), peak (t=0) nonlinear phase shift with the sample at focus (Z=0).

$\Delta\Phi_{Z0}=(2\pi/\lambda)n_2I_0Z_0$

Δn : change in index of refraction

Δn_0 : peak-on-axis change of refractive index

$\Delta T(Z)$: normalized transmittance of the sample when at position Z, $\Delta T(Z)=T(Z)/T(Z>>Z_0)$

ΔT_{pv} : change in normalized transmittance between peak and valley, $|T_p-T_v|$

ΔZ_{pv} : distance between the Z positions of the peak and valley

σ : excited-state absorption cross section

σ_r : excited-state refractive cross section

$\chi^{(3)}$: third-order nonlinear electric susceptibility

$\chi^{(5)}$: fifth-order nonlinear electric susceptibitlity

d : distance between the focal position and the far-field aperture

E_a : electric field at the aperture (see Eq. 17)

ESA : excited-state absorption

f(t) : temporal profile of the incident pulse

F : fluence (energy per unit area)

FOM : figure of merit

F(x,l) : Normalized transmittance function for thick medium

I : irradiance (power per unit area)

I_0 : peak on-axis irradiance at the focus

I_{sat} : saturation irradiance

k_0 : wave number in vacuum

L : sample length

L_{eff} : $(1-e^{-\alpha L})/\alpha$ used for a third-order nonlinearity

L'_{eff} : $(1-e^{-2\alpha L})/2\alpha$ used for a fifth-order nonlinearity

l : L/Z_0

l_{eff} : $L_{eff}(thick)/Z_0=\Delta T_{pv}(thick)/(0.406\Delta\Phi_{z0})$

n : index of refraction

n_2 : third-order nonlinear refractive index ($\Delta n=n_2 I$)

n_4 : fifth-order nonlinear refractive index so that $\Delta n=n_4 I^2$

q : $\beta I L_{eff}$

q_0 : $\beta I_0 L_{eff}$

r : radial coordinate

RSA : reverse -saturable absorption (ESA, a cumulative effect)

S : fraction transmitted by the aperture in the Z-scan (S is the fraction blocked by the disk in an EZ-scan)

t : time

T(Z) : the sample transmittance when at position Z

T_p : normalized sample transmittance when situated at the position of maximum transmittance (peak)

T_v : normalized sample transmittance when situated at the position of minimum transmittance (valley)

w_0 : Gaussian beam spot radius at focus (half width at $1/e^2$ of maximum of the irradiance)

x : Z/Z_0 position of the sample with respect to focal plane

X_p : Z/Z_0 position of the peak transmittance for a thick sample Z-scan

X_v : Z/Z_0 position of the valley transmittance for a thick sample Z-scan

z : depth within the sample

Z : position of the sample with respect to the focal position

Z_0 : Rayleigh range equal to $n\pi w_0^2/\lambda$

TABLE OF CONTENTS

1. Introduction

There is considerable interest in finding materials having large yet fast nonlinearities. This interest, that is driven primarily by the search for materials for all-optical switching and sensor protection applications, concerns both nonlinear absorption (NLA) and nonlinear refraction (NLR). The database for nonlinear optical properties of materials, particularly organic, is in many cases inadequate for determining trends to guide synthesis efforts. Thus, there is a need to expand this database. Methods to determine nonlinear coefficients are discussed throughout this book. The Z-scan technique is a method which can rapidly measure both NLA and NLR in solids, liquids and liquid solutions.[1,2] In this chapter we first present a brief review of this technique and its various derivatives. Simple methods for data analysis are then discussed for "thin" and "thick" [3,4,5,6] nonlinear media Z-scans, eclipsing Z-scan (EZ-scan) [7], two-color Z-scans [8,9], time-resolved excite-probe Z-scans [10,11], and top-hat-beam Z-scans [12]. Finally, an overview of the reported measurements of the nonlinear optical properties of organic materials as determined using these techniques will be presented .

The Z-scan method has gained rapid acceptance by the nonlinear optics community as a standard technique for separately determining the nonlinear changes in index and changes in absorption. This acceptance is primarily due to the simplicity of the technique as well as the simplicity of the interpretation. In most experiments the index change, Δn, and absorption change, $\Delta\alpha$, can be determined directly from the data without resorting to computer fitting. However, it must always be recognized that this method is sensitive to all nonlinear optical mechanisms that give rise to a change of the refractive index and/or absorption coefficient, so that determining the underlying physical processes present from a Z-scan is not in general possible. A series of Z-scans at varying pulsewidths, frequencies, focal geometries etc. along with a variety of other experiments are often needed to unambiguously determine the relevant mechanisms. In this regard, we caution the reader that the conclusions as to the active nonlinear processes of any given reference using the Z-scan technique is often subject to debate.

2. Technique and Simple Relations

The standard "closed aperture" Z-scan apparatus (i.e. aperture in place in the *far field*) for determining nonlinear refraction is shown in Fig. 1. The transmittance of the sample through the aperture is monitored in the far field as a function of the position, Z, of the nonlinear sample in the vicinity of the linear optics focal position. The required scan range in an experiment depends on the beam parameters and the sample thickness L. A critical parameter is the diffraction length, Z_0, of the focused beam defined as $\pi w_0^2/\lambda$ for a Gaussian beam where w_0 is the focal spot size (half-width at the $1/e^2$ maximum in the irradiance). For "thin" samples (i.e. $L \leq Z_0$), although all the information is theoretically contained within a scan range of $\pm Z_0$, it is preferable to scan the sample for $\approx \pm 5Z_0$ or more. This requirement, as we shall see, simplifies data interpretation when the sample's surface roughness or optical beam imperfections introduce background "noise" into the measurement system. In many practical cases where considerable laser power fluctuations may occur during the scan, a reference detector can be used to monitor and normalize the transmittance (see Fig.1). To eliminate the possible noise due to spatial beam fluctuations, this reference arm can be further modified to include a lens and an aperture identical to those in the nonlinear arm [9]. The position of the aperture is rather arbitrary as long as its distance from the focus, $d >> Z_0$. Typical values range from $20Z_0$ to $100Z_0$. The size of the aperture is signified by its transmittance, S, in the linear regime, i.e. when the sample has been placed far away from the focus. In most reported experiments, $0.1<S<0.5$ has been used for determining nonlinear refraction. Obviously, the S=1 case corresponds to collecting all the transmitted light and therefore is insensitive to any nonlinear beam distortion due to nonlinear refraction. Such a scheme, referred to as an "open aperture" Z-scan, is suited for measuring nonlinear absorption ($\Delta\alpha$) in the sample. We will discuss this in more detail later.

A typical closed aperture Z-scan output for a thin sample exhibiting nonlinear refraction, is shown in Fig. 2 (solid line). For example, a self-focusing nonlinearity, $\Delta n>0$, results in a valley followed by a peak in the normalized transmittance as the sample is moved away from the lens in Fig. 1 (increasing Z). The normalization is performed in such a way that the transmittance is unity for the sample far from focus where the nonlinearity is negligible (i.e. for $|Z| >> Z_0$). The positive lensing in the sample placed before the focus moves the focal position closer to the sample resulting in a greater far field divergence and a reduced aperture transmittance. On the other hand, with the sample placed after focus, the same positive lensing reduces the far field divergence allowing for a larger aperture transmittance. The opposite occurs for a self-defocusing nonlinearity, $\Delta n<0$ (Fig.2, dashed line).

One of the attractive features of the Z-scan technique is the ease and simplicity by which the nonlinear optical coefficients can be determined with a high degree of accuracy. However, as is the case with most nonlinear optical measurement

techniques, the measured quantities are the nonlinearly induced $<\Delta n>$ and/or $<\Delta\alpha>$, where $< >$ denotes the time-average over a time corresponding to the temporal resolution of the detection system. Accurate determination of the nonlinear coefficients such as n_2 or β depends on competing nonlinearities, and therefore depend on the model, and on how precisely the laser source is characterized in terms of its temporal and spatial profiles, power or energy content and stability.

Once a specific type of nonlinearity is assumed (e.g. an ultrafast $\chi^{(3)}$ response), a Z-scan can be rigorously modeled for any beam shape and sample thickness by solving the appropriate Maxwell's equations. However, a number of valid assumptions and approximations will lead to simple analytical expressions, making data analysis easy yet precise. Aside from the usual SVEA (slowly varying envelope approximation, a major simplification results when we assume the nonlinear sample is "thin" so that neither diffraction nor nonlinear refraction cause any change of beam profile within the nonlinear sample. This implies that $L<<Z_0$ and $L<<Z_0/\Delta\Phi_0$ respectively where $\Delta\Phi_0$ is the maximum nonlinearly-induced phase distortion. The latter requirement assures "external self-action" and simply states that the effective focal length of the induced nonlinear lens in the sample should be much smaller then the sample thickness itself.[13] In most experiments using the Z-scan technique we find that this second criterion is automatically met since $\Delta\Phi_0$ is small. In section 4 we will analyze thick sample Z-scans ($L>Z_0$) and show that for small enough phase distortions simple expressions can still be derived for the Z-scan transmittance. Additionally we will show that for the sample to be safely regarded as "thin", the first criterion for linear diffraction is more restrictive than it need be, and it is sufficient to replace it with $L\leq Z_0$.

The external self action limit simplifies the problem considerably, and the amplitude $\sqrt{I}$ and phase $\Delta\phi$ of the electric field *E* are now governed in the SVEA by the following pair of simple equations*:*

$$\frac{d\Delta\phi}{dz'} = \frac{2\pi}{\lambda}\Delta n(I) \quad (1)$$

and

$$\frac{dI}{dz'} = -\alpha(I)I, \quad (2)$$

where z' is the propagation depth in the sample and $\alpha(I)$ in general includes linear and NLA terms. Note that z' should not be confused with the sample position Z.

For third-order nonlinearities we take,

$$\Delta n = \left\{\frac{n_2}{2}|E|^2\right\}_{esu} = \{n_2 I\}_{MKS} \quad (3)$$

and

$$\Delta\alpha = \beta I, \quad (4)$$

where n_2 is the nonlinear index of refraction, *E* is the peak electric field (cgs), and *I* denotes the irradiance (MKS) of the laser beam within the sample. Here β denotes the third-order nonlinear absorption coefficient, which for ultrafast NLA is equal to the two-photon absorption (2PA) coefficient. n_2(esu) and n_2(MKS) are related through the conversion formula, $n_2(esu)=(cn_0/40\pi)n_2(MKS)$, where c (m/sec) is the speed of light in vacuum. We note, however, that while we are using n_2 here for *any* third order nonlinearity, it may not be the best description of cumulative nonlinearities. These occur in, for example, reverse saturable absorbing (RSA) dyes.[14] In such dyes linear absorption is followed by excited-state absorption (ESA) where the excited-state cross section is larger than the ground-state cross section. As the resulting change in absorption is best described by a cross section and not by a two-photon absorption coefficient, the index change, here due to population redistribution, is better described by refractive cross sections than by an n_2. Such an "n_2" (or β) would change with the laser pulsewidth. [15,16] This is discussed in more detail in Sec. 5.

Once the amplitude and the phase of the beam exiting the sample are known, the field distribution at the far-field aperture can be calculated using diffraction theory (Huygen's principle). We will briefly review this procedure in Sec. 3 for a Gaussian beam. Simple analytical or empirical relations as obtained from those rigorous treatments will be presented in this section. In most practical cases these relations present a convenient yet accurate method for estimating the nonlinear coefficients. In the remainder of this chapter n_2 always refers to n_2 (MKS).

2.1 Nonlinear Refraction ($\Delta\alpha=0$)

We define the change in transmittance between the peak and valley in a Z-scan as $\Delta T_{pv}= T_p - T_v$ where T_p and T_v are the normalized peak and valley transmittances as seen in Fig. 2. The empirically determined relation between the induced phase distortion, $\Delta\Phi_0$, and ΔT_{pv} for a third-order nonlinear refractive process in the absence of NLA is,

$$\Delta T_{pv} \cong 0.406(1-S)^{0.27}\left|\Delta\Phi_0\right|, \quad (5)$$

where

$$\Delta\Phi_0 = \frac{2\pi}{\lambda} n_2 I_0 L_{eff} \quad (6)$$

with, $L_{eff}=(1-e^{-\alpha L})/\alpha$, and S is the transmittance of the aperture in the absence of a sample. $\Delta\Phi_0$ and I_0 are the on-axis (r=0), peak (t=0) nonlinear phase shift and the irradiance with the sample at focus (Z=0) respectively. The sign of $\Delta\Phi_0$ and hence n_2 is determined from the relative positions of the peak and valley with Z as shown in Fig. 2. This relation is accurate to within ±3% for $\Delta T_{pv} < 1$. As an example, if the induced optical path length change due to the nonlinearity is $\lambda/250$, ΔT_{pv} ≈1% for an aperture transmittance of S=0.4. Use of S=0.4 is a good compromise between having a large signal which averages possible beam nonuniformities, thus reducing background signals, and loss of sensitivity.

A useful feature of the Z-scan trace is that the Z-distance between peak and valley, ΔZ_{pv}, is a direct measure of the diffraction length of the incident beam for a given nonlinear response. In an standard Z-scan (i.e. using a Gaussian beam and a far-field aperture), this relation for a third-order nonlinearity is given by:

$$\left|\Delta Z_{pv}\right| \approx 1.7 Z_0 \quad (7)$$

For small $\Delta\Phi_0$, peak and valley are equidistant (≈±0.856 Z_0) from the focus (Z=0). As $\Delta\Phi_0$ increases, the peak and valley positions do not remain symmetric; the valley moving toward focus and the peak away so that ΔZ_{pv} remains nearly constant as given above. Being independent of the irradiance, this relation is quite helpful in estimating Z_0 and hence the beam waist w_0, of the focused beam. We must re-emphasize that the above relation is valid only for closed-aperture Z-scans involving an n_2-type nonlinearity, a good quality Gaussian beam (M^2≈1), and thin nonlinear samples. Any departure from these conditions will give rise to a different characteristic ΔZ_{pv}. Later on, we will briefly discuss cases involving thick samples, $\chi^{(5)}$-type nonlinearities, eclipsing and top-hat-beam Z-scans.

The linear relationship between ΔT_{pv} and $\Delta\Phi_0$ makes it convenient to include a time averaging factor which is not included in Eqs. 5 and 6 for pulsed inputs. Inclusion of this temporal averaging reduces the measured ΔT_{pv} by a factor, A_τ, which generally depends on the pulse shape and the response time of the nonlinearity. For nonlinearities with response times much shorter than the pulsewidth (i.e. instantaneous nonlineariteis), A_τ is given by: [2]

$$A_\tau = \frac{\int_{-\infty}^{+\infty} f^2(t)dt}{\int_{-\infty}^{+\infty} f(t)dt}, \quad (8)$$

where *f(t)* denotes the temporal profile of the incident laser pulse. For a Gaussian temporal shape, this gives $A_\tau=\sqrt{2}$ while a *Sech*^{2} pulse gives $A_\tau=2/3$. In the other extreme, where the time response of the nonlinearity is much larger then the pulsewidth, A_τ assumes a value of 1/2 for a third-order nonlinearity, independent of the pulse shape [2]. Of course, in this case, the interpretation of n_2 changes. For example, in the case of reverse-saturable absorbers and under the

approximations discussed in Ref. [16], $n_2 I_0$ is replaced by $\sigma_r F/2\hbar\omega$, where σ_r is the excited-state refractive cross section. Cases involving higher-order nonlinearities, and/or with response times that are comparable to the pulsewidth, require proper averaging of $\Delta\Phi_0(t)$ according to Eq. 8, and will not be discussed here.

2.2 Higher Order Nonlinearities:

Although many observed nonlinear optical effects give index changes proportional to the irradiance ($\Delta n \propto I$), we often encounter higher order effects where $\Delta n \propto I^{\eta}$, with $\eta>1$. For example, a fifth order NLR, (a $\chi^{(5)}$-type nonlinearity where $\eta=2$) becomes the dominant mechanism in semiconductors when Δn is induced by two-photon generated free-carriers. [17] For this type of nonlinearity, where $\Delta n = n_4 I^2$ is assumed, we can derive simple relations that accurately characterize the Z-scan data. For a Gaussian beam and far-field aperture, these are given by:

$$\Delta T_{pv} \cong 0.21(1-S)^{0.27}\left|\Delta\Phi_0\right|, \quad (9)$$

and

$$\left|\Delta Z_{pv}\right| \approx 1.2 Z_0, \quad (10)$$

where $\Delta\Phi_0 = k n_4 I_0^2 L'_{eff}$ with $L'_{eff} = [1-\exp(-2\alpha L)]/2\alpha$. In certain cases where competing $\chi^{(3)}$ and $\chi^{(5)}$ processes are simultaneously involved, the data analysis becomes more complicated. In Ref. [17] a procedure is given for separating the two processes using a number of Z-scans at different irradiances. This procedure makes use of simple relations of eqns. (5) and (9) to estimate the nonlinear coefficients associated with both $\chi^{(3)}$ and $\chi^{(5)}$ processes.

2.3 Eclipsing Z-scan (EZ-Scan)

As the Z-scan method relies on propagation of a phase distortion to produce a transmittance change, the minimum detectable signal is determined by how small a transmittance change can be measured. The surprising interferometric sensitivity comes about from the interference (diffraction) of different portions of the spatial profile in the far field. Recently, it was realized that this sensitivity could be greatly increased by looking at the outer edges of the beam in the far field rather than the central portion as in the Z-scan. This is accomplished by replacing the apertures in Fig. 1 with disks that block the central part of the beam. The light that leaks around the edges appears as an eclipse, thus the name EZ-scan for eclipsing Z-scan.[7] An analogous empirical expression to Eq. 9 for the EZ-scan is

$$\Delta T_{pv} \cong 0.68(1-S)^{-0.44}\left|\Delta\Phi_0\right|, \quad (11)$$

which is accurate to within ±3% for $|\Delta\Phi_0| \le 0.2$ and a disk linear transmittance rejection S in the range $0.98>S>0.995$, i.e. the fraction of light seen by the detector is 1-S. Figure 3 shows a comparison of an EZ-scan with a Z-scan for a phase distortion of 0.1 radian for S=0.02. The relative positions of peak and valley switch from the Z-scan since light that is transmitted by an aperture is now blocked by the disk and vise versa. Evident from the above relation, as $S\rightarrow 1$ (large disks), the sensitivity increases significantly. Sensitivities to optical path length changes of $\cong\lambda/10^4$ have been demonstrated as compared to $\cong\lambda/10^3$ for Z-scan. For the range of S given above, the spacing between peak and valley, ΔZ_{pv}, is empirically found to be given by $\Delta Z_{pv} \approx 0.9\text{-}1.0 Z_0$, which grows to the Z-scan value of $\approx 1.7 Z_0$ as $S\rightarrow 0$. The enhancement of sensitivity in the EZ-scan , however, comes at the expense of signal photons as well as a reduction in accuracy and absolute calibration capability. This added uncertainty originates from the deviations of the actual laser beams from a Gaussian distribution, and the fact that we need to know S very accurately. We, therefore, recommend using this technique only when the added sensitivity is required and with a known reference sample to calibrate the system.

2.4 Nonlinear Absorption

While NLA can be determined using a two parameter fit to a closed aperture Z-scan (i.e. fitting for both Δn and $\Delta\alpha$), it is more directly (and more accurately) determined in an open aperture Z-scan. For small third-order nonlinear losses, i.e. $\Delta\alpha L=\beta I L_{eff}<<1$ with response times much less than the pulsewidth (e.g. two-photon absorption), and for a Gaussian temporal shape pulse, the normalized change in transmitted energy $\Delta T(=T(Z)-1)$ becomes

$$\Delta T(z) \approx -\frac{q_0}{2\sqrt{2}} \frac{1}{[1+Z^2/Z_0^2]}\ , \quad (12)$$

where $q_0 =\beta I_0 L_{eff}$ ($|q_0|<<1$). This mimics the Lorentzian distribution of the irradiance with Z for a focused Gaussian beam as seen in Fig. 4. If the response time of the material is much longer than the pulsewidth used, the factor $2\sqrt{2}$ is replaced by 2. This is independent of the temporal pulse shape. Of course, in this case, the interpretation of β changes. For example, in the case of reverse-saturable absorbers and under the approximations discussed in Ref. [16], βI_0 is replaced by $\sigma F/2\hbar\omega$, where σ is the excited-state absorption cross section.

2.5 Nonlinear Refraction in the Presence of Nonlinear Absorption ($\Delta\alpha\neq0$)

We can also determine NLR in the presence of NLA. This can be done by fitting the Z-scan with a two parameter fit or by separately measuring the NLA in a Z-scan performed with the aperture removed (i.e. open aperture Z-scan). This second method is more accurate since two single parameter fits give a higher accuracy than one two parameter fit. Within approximations elaborated in Ref. **2** (primarily that the Z-scan is not dominated by nonlinear absorption) a simple division of the curves obtained from the two Z-scans (closed/open) gives a curve that closely approximates what would be obtained with a closed aperture Z-scan on a material having the same Δn but with $\Delta\alpha=0$. This greatly simplifies determining Δn. An example of this division process is shown in Fig. 5. In lieu of this division, with $\Delta\alpha$ known from the open aperture results, the Z-scan with aperture in place ($S<1$) can be used to extract the remaining unknown, namely Δn.[17]

2.6 Excite-Probe Z-scans

Excite-probe techniques in nonlinear optics have been commonly employed in the past to deduce information that is not accessible with a single beam geometry. The most significant application of such techniques concerns the ultrafast dynamics of the nonlinear optical phenomena. There has been a number of investigations that have used Z-scan in an excite-probe scheme.[8,9,10,11] The general geometry is shown in Fig. 6 where collinearly propagating excitation and probe beams are used. After propagation through the sample, the probe beam is then separated and analyzed through the far-field aperture. Due to collinear propagation of the excitation and probe beams, we are able to separate them only if they differ in wavelength or polarization. The former scheme, known as a 2-color Z-scan, has been used to measure the nondegenerate n_2 and β in semiconductors.[8,9] The time-resolved studies can be performed in two fashions. In one scheme, Z-scans are performed at various fixed delays between excitation and probe pulses. In the second scheme, the sample position is fixed (e.g. at the peak or the valley positions) while the transmittance of the probe is measured as the delay between the two pulses is varied. The analysis of the 2-color Z-scans is naturally more involved than that of a single beam Z-scan. The measured signal, in addition to being dependent on the parameters discussed for the single beam geometry, will also depend on parameters such as the excite-probe beam waist ratio, pulsewidth ratio and the possible focal separation due to chromatic aberration of the lens.[8,10]

2.7 Z-scans with Non-Gaussian Beams

While Gaussian beams are extremely convenient since their propagation is particularly simple (e.g. a Gaussian beam remains Gaussian throughout a linear optical system in the absence of aberrations), the output of many lasers do not posses a Gaussian profile in space. Zhao and Palffy-Muhoray[12] derived the results of performing a Z-scan using a focused "top-hat" beam, where the profile at the initial focusing lens is approximately a step function (Heaviside function) in the radial coordinate r (i.e. $\Theta(r_0-r)$ with r_0 a constant). In practice, one can produce this type of beam profile by sufficiently expanding any spatially coherent optical beam and then use a circular aperture at the focusing lens. The lens focuses this beam to an Airy pattern in the absence of aberrations. The emprical expression relating ΔT_{pv} to $\Delta\Phi_0$ and aperture transmittance S is given by: [12]

$$\Delta T_{pv} \approx 2.8(1-S)^{1.14} \tanh(0.37\Delta\Phi_0) \ , \quad (13)$$

where $\Delta\Phi_0$ is the peak nonlinear phase shift at the center of the Airy disk at the focal plane. For S≈0 and small $\Delta\Phi_0$, the above expression gives $\Delta T_{pv} \approx 1.036\Delta\Phi_0$, indicating approximately a 2.5 times larger sensitivity than for a Gaussian beam Z-scan. This enhanced sensitivity is due to the steeper beam curvature gradients encountered by the nonlinear sample at Z positions near the focal plane.

It is also possible to use a sample of known nonlinearity as a reference to calibrate a system using a beam of arbitrary profile. Reference[18] shows a way to use a reference sample to obtain the relative NLA and NLR without regard to the laser beam characteristics. This also allows violation of the thin sample approximation as long as the reference sample has the same thickness as the sample under measurement, and the irradiance is adjusted such that the ΔT_{pv}'s in both measurements are nearly equal. More generally, Z-scans using reference sample calibration are useful provided that the orders of both nonlinearities are the same (e.g. both are $\chi^{(3)}$ type) and conditions and parameters of both experiments are kept nearly the same.

2.8 Background Subtraction

In all the possible situations discussed above, it is often beneficial to perform experiments at high and low irradiance levels (low enough that the nonlinear response is negligible) and subtract the two sets of data.[2] This greatly reduces background signals due, for example, to sample inhomogeneities or sample wedge. A necessary condition for this background subtraction process to be effective is that the sample position be reproducible for both high and low irradiance scans (i.e. laterally, vertically and along Z). It is also important that the data sets be normalized before subtraction such that T(|Z|>>Z0) are made equal for high and low irradiance Z-scans. Experience shows that even when the signal is indistinguishable in a background that this subtraction can often uncover a usable signal.[2]

3. Analysis of Z-scan for a Thin Nonlinear Medium

While the above analysis gives the dependence of NLA on the sample position Z, the analysis for NLR was restricted to ΔT_{pv}. The Z dependence for NLR can be obtained by straightforward numerical techniques as outlined below. [2] We find it useful to fit the full Z dependence of the Z-scan signals since there is information regarding the order of the nonlinearity in this Z dependence as discussed in Section 1.

The irradiance distribution and phase shift of the beam at the exit surface of a sample exhibiting a third-order nonlinear refractive index are obtained by simultaneously solving Eqs. 1 and 2:

$$I_e(Z,r,t) = \frac{I(Z,r,t)\exp^{-\alpha L}}{1+q(Z,r,t)}, \quad (14)$$

and

$$\Delta\phi(Z,r,t) = \frac{kn_2}{\beta}\ln[1+q(Z,r,t)] \quad (15)$$

where $q(Z,r,t)=\beta I(Z,r,t)L_{eff}$. Combining Eqs. 14 and 15 we obtain the complex field at the exit surface of the sample to be [2,4]

$$E_e = E(Z,r,t)e^{-\alpha L/2}(1+q)^{(ikn_2/\beta-1/2)} \ , (16)$$

where *E(Z,r,t)* is the incident electric field. The reflection losses can be safely assumed to be linear and hence will be ignored in this formalism. In evaluating the nonlinear coefficients, however, one should account for reflection loss of the first surface by taking the irradiance (i.e. I_0) to be that of the inside of the sample.

In general for radially symmetric systems, a zeroth order Hankel transform of Eq. 16 will give the field distribution E_a at the aperture which is placed a distance *d* from the focal plane:

$$E_a(Z,r,t,d) = \frac{2\pi}{i\lambda\, d'}\exp\left(\frac{i\pi r^2}{\lambda\, d'}\right)\int_0^\infty r'dr'\ E_e(Z,r',t-d'/c)\exp\left(\frac{i\pi\, r'^2}{\lambda\ d'}\right) J_0\left(\frac{2\pi r r'}{\lambda\, d'}\right) \quad (17).$$

where d'=d-Z is the distance from the sample to the aperture plane. The measured quantity is the pulse energy or average power transmitted through the far-field aperture having a radius of r_a. The normalized transmittance is then obtained as:

$$T(Z) = \frac{\int_{-\infty}^{\infty} dt \int_0^{r_a} |E_a(Z,r,t,d)|^2\, r dr}{U} \qquad (18),$$

where U is the same as the numerator but in the linear regime (i.e. for I≈0). In the case of an EZ-scan, the limits of the spatial integral in Eq. 18 must be replaced by r_d to ∞ where r_d is the radius of the obscuration disk. It is generally more convenient to represent the aperture (or disk) size by the normalized transmittance (or rejection) S in the linear regime.

The formalism thus far presented is generally applicable to any radially symmetric beam. Here, however, we assume a $TEM_{0,0}$ Gaussian distribution for the incident beam as given by:

$$E(Z,r,t) = E_0(t)\frac{w_0}{w(Z)}.\exp\left(-\frac{r^2}{w^2(Z)} + i\frac{\pi r^2}{\lambda R(Z)} + i\phi\right), \quad (19)$$

where $w(Z)=w_0(1+Z^2/Z_0^2)^{1/2}$ and $R(z)= Z+Z_0^2/Z$. The radially invariant phase terms, contained in ϕ, are immaterial to our calculations and hence will be ignored.

The integral in Eq. 17 can be analytically evaluated if we assume that |q|<1 (in Eq. 16) and then perform a binomial series expansion of E_e in powers of q. Recalling that $q \propto I \propto \exp(-r^2/w^2)$, this expansion effectively decomposes E_e into a sum of Gaussian beams with varying beam parameters. This method of beam propagation known as Gaussian decomposition was first given by Wearie et. al.[19] Following the expansion, we obtain:

$$E_e = E(Z,r,t)e^{-\alpha L/2}\sum_{m=0}^{\infty} F_m \exp(2mr^2 / w^2(Z)), \quad (20)$$

where the F_m, the factor containing the nonlinear optical coefficients, is given by:

$$F_m = \frac{(i\Delta\phi_0(Z,t))^m}{m!}\prod_{j=1}^{m}\left[1 + i\left(j - \frac{1}{2}\right)\frac{\lambda\beta}{2\pi n_2}\right], \quad (21)$$

with $F_0=1$ and $\Delta\phi_0(Z,t)=\Delta\phi(Z,r=0,t)$ denoting the on-axis instantaneous nonlinear phase shift . The Hankel transform of E_e will then give the field at the aperture plane as a sum of Gaussian beams:

$$E_a(r,t) = E(Z,r=0,t)e^{-\alpha L/2}\sum_{m=0}^{\infty} F_m \frac{w_{m0}}{w_m}\exp\left[-\frac{r^2}{w_m^2} + \frac{i\pi r^2}{\lambda R_m} + i\theta_m\right], \quad (22)$$

where the beam parameters of each Gaussian beam are as follows:

$$w_{m0}^2 = \frac{w^2(Z)}{2m+1}, \quad d_m = \frac{k w_{m0}^2}{2}, \quad w_m^2 = w_{m0}^2\left[g^2 + \frac{d^2}{d_m^2}\right], \quad R_m = d\left[1 - \frac{g}{g^2 + d^2/d_m^2}\right]^{-1}, \text{ and}$$

$$\theta_m = \tan^{-1}\left[\frac{g}{d/d_m}\right], \text{ where } g = 1 + d/R(Z) \qquad (23)$$

Finally, the normalized transmittance can then be evaluated as given by Eq. (18). We should note here that with an incident Gaussain beam, the aperture transmittance can be given as $S=1-\exp(-2r_a^2/w_a^2)$ where $w_a=w_0(1+d^2/Z_0^2)^{1/2}$ is the linear beam radius at the aperture.

It is worthwhile to analyze the implications of the above results under a number of further approximations. In the absence of nonlinear absorption (i.e. β=0), $F_m = (i\Delta\phi_0(Z,t))^m / m!$ and the far-field beam deformation will be as a result of external self-action (self-focusing and self-defocusing). In that case we can write $\Delta\phi_0$ as:

$$\Delta\phi_0(Z,t) = \frac{2\pi}{\lambda} L_{eff} n_2 I(Z,t) = \Delta\Phi_0 \frac{f(t)}{1+Z^2/Z_0^2}, \quad (24)$$

where $\Delta\Phi_0=\Delta\phi_0(0,0)$ is the peak-on-axis nonlinear phase shift, and f(t) represents the irradiance temporal profile of the incident pulse. We find that this Gaussian decomposition method is very useful for the small phase distortions detected with the Z-scan (or EZ-scan) method since only a few terms of the sum in Eq. 22 are needed. Figure 2 depicts calculated Z-scans for $\Delta\Phi_0=\pm 0.5$ using the above formalism.. The simple relations (Eq. 9 and 11) given earlier were obtained by empirically fitting the calculated results using the equations derived in this section. As was shown in Ref.[2], such emprical relations are exact in the limit of small $\Delta\Phi_0$ where only one nonlinear term in the expansion (Eq. 22) is retained.

With NLA present (i.e. β≠0), although no restriction is imposed on the magnitude of $\Delta\Phi_0$, the above formalism is valid only for $q_0=|\beta I_0 L_{eff}|<1$. Note that the coupling factor $\lambda\beta/2\pi n_2 = q_0/\Delta\Phi_0$ in Eq.(21) is twice the ratio of the imaginary to real parts of the third-order nonlinear susceptibility, $\chi^{(3)}$ (i.e. $q_0/2\Delta\Phi_0 = \mathrm{Im}\{\chi^3\}/\mathrm{Re}\{\chi^3\}$). The 2PA figure-of-merit (FOM) for all-optical switching has been defined as 4π times this value.[20] Since the irradiance and effective length cancel in this ratio, this FOM can be deduced for third-order nonlinearities without knowledge of the irradiance or sample length as long as the thin sample approximation in valid.

The Z-scan transmittance variations can be calculated following the same procedure as described previously. As is evident from Eqs. 21-22, the absorptive and refractive contributions to the far field beam profile and hence to the Z-scan transmittance are coupled. When the aperture is removed, however, the Z-scan transmittance is insensitive to beam distortion and is only a function of the nonlinear absorption. The total transmitted fluence in that case (S=1) can be obtained by spatially integrating Eq. 14 without having to include the free space propagation process. The resultant normalized transmittance for a pulse with a temporal profile $f(t)$ can be then derived as: [2]

$$T(Z,S=1) = \frac{1+Z^2/Z_0^2}{q_0} \frac{\int_{-\infty}^{+\infty} \ln\left[1+q_0\frac{f(\tau)}{1+Z^2/Z_0^2}\right] d\tau}{\int_{-\infty}^{+\infty} f(\tau)\,d\tau}. \quad (25)$$

For $|q_0|<1$, this transmittance can be expressed in terms of the peak irradiance in a summation form more suitable for numerical evaluation. Assuming a Gaussian temporal profile (i.e. $f(\tau)=\exp(-\tau^2)$) this can be written as :

$$T(Z,S=1) = \sum_{m=0}^{\infty} \frac{(-q_0)^m}{(1+Z^2/Z_0^2)^m (m+1)^{3/2}}, \quad (26)$$

Thus, once an open aperture (S=1) Z-scan is performed, β can be unambiguously deduced. With β known, the Z-scan with aperture in place (S<1) can be used to extract the remaining unknown, namely the coefficient n_2. Note that ΔT, as given by Eq. 12 in section 1, is simply the m=1 term in Eq. (26).

4. Z-scan for "Thick" samples

It is apparent from relations derived so far, that a way to obtain larger Z-scan signals (ΔT_{pv}) is to increase $\Delta\Phi_0$ through either stronger focusing (shorter Z_0) or thicker samples (larger L) . In either case, we recall that the validity of these relations becomes questionable once the *thin* sample criterion ($L \ll Z_0$) is violated. In this section we address this problem and analyze a general case in which no limitation is imposed on the sample length. The rigorous treatment of this problem involves numerical solutions to nonlinear wave equations and will not be discussed here.[6] In addition to numerical calculations, two types of approximate solutions, resulting in simple relations, have been reported. One involves an "aberration-free" approximation of the nonlinear wave equation,[3,21] and the other treats the wave propagation exactly to first order in the nonlinear phase shift (Δϕ).[4,5] The latter approach requires that Δϕ is small enough that no nonlinear beam

distortion (self-action) occurs within the sample although linear diffraction does occur. This condition is controllable and can be satisfied in an experiment. In fact, often being faced with this limitation (low Δn), is the very reason that one resorts to thick sample conditions.

Following Hermann and McDuff [4], and Tian et al.[5], the on-axis ($S\approx 0$) Z-scan transmittance of a *thick* nonlinear sample can be written as:

$$T(x) \approx 1 + \Delta\Phi_{z_0} F(x,l), \quad (27)$$

where $\Delta\Phi_{z0} = (2\pi/\lambda) n_2 I_0 Z_0$ is the nonlinear phase shift occurring within one Z_0, $x = Z/Z_0$, and $l = L/Z_0$ is the normalized length of the sample. Here, for simplicity, we assume that the linear refractive index, $n_0 = 1$. *F(x,l)* is given by:[4]

$$F(x,l) = \frac{1}{4}\ln\left(\frac{\left[(x+l/2)^2+1\right]\left[(x-l/2)^2+9\right]}{\left[(x-l/2)^2+1\right]\left[(x+l/2)^2+9\right]}\right). \quad (28)$$

Plots of *F(x,l)*are shown in Fig. 7 for l=1,2,5,8,and 10. The position of peak and valley are obtained by evaluating *dF/dx=0*, which gives:

$$X_{p,v} = \pm\sqrt{\frac{(l^2/2 - 10) + \sqrt{(l^2+10)^2 + 108}}{6}}, \quad (29)$$

The peak-valley separation, therefore, is given by $\Delta Z_{pv} = 2|X_{p,v}|Z_0$. As evident from Fig. 8 which shows L_{eff}/Z_0 as a function of L/Z_0, this separation approaches *L (or L/*n_0) for $L >> Z_0$.[3] All the above relations reduce to that derived for a thin sample when we let $l \to 0$. Moreover, as one would expect, it is seen in Fig 8 that by increasing the sample thickness above $\approx 2Z_0$, the signal (ΔT_{pv}) gradually levels off and ultimately becomes a constant. A useful quantity that illustrates this effect, is the effective length of a thick nonlinear medium defined as the length that can be attributed to the sample if it were to be regarded as thin in data analysis. Once we identify such an effective length, we can use the "thin" sample relation (Eq. 5) to quickly evaluate the n_2 coefficient for third-order nonlinearities. We, thus, define this length as $l_{eff} = L_{eff}/Z_0 = \Delta T_{pv}(\text{thick})/(0.406\Delta\Phi_{z0})$ [3] which is evaluated from the above expressions as:

$$l_{eff} = \frac{F(|X_{p,v}|, l)}{2 \times 0.406}. \quad (30)$$

This is plotted in Fig. 8 together with a simpler empirical fit given by:

$$l_{eff} = \frac{2.706[(l+1)^{1.44} - 1]}{l^{1.44} + 3.924}. \quad (31)$$

In an actual experiment where $n_0 > 1$, the above expressions should be modified by simply replacing Z_0 with $n_0 Z_0 = n_0 \pi w_0^2/\lambda$. This substitution, however, will not account for the longitudinal shift of the linear focus. But since no useful information (regarding the nonlinear optical measurement) exists in the absolute position of the transmittance peak and valley, the above procedure is sufficient and simple.

5. Interpretation

There are many physical processes which can lead to third-order nonlinearities (i.e. effects proportional to the input irradiance, fluence or energy). Ultrafast nonlinear absorption processes include multiphoton absorption[22,23], stimulated Raman scattering[24] and AC-Stark effects.[25,26] These lead via causality and Kramers-Kronig relations to the bound-electronic nonlinear refractive index, n_2.[25,26,27,28] Cumulative (i.e. slow) nonlinearities include population redistribution from linear absorption (this includes saturable and excited-state or reverse saturable absorption and their refractive counterparts), reorientation of anisotropic molecules such as in CS_2, thermal refraction, electrostriction, etc. The Z-scan is sensitive to all of these nonlinearities including higher-order effects and cannot simply be used by itself to distinguish these nonlinear processes or separate fast from slow nonlinearities.

A key to distinguishing these processes is to pay particular attention to the temporal response. Ultrafast nonlinearities are easily analyzed as has been discussed. The use of pulsewidths much shorter than the decay times of excited states allows such cumulative nonlinearities to be more easily analyzed. As we shall show, in this regime, the excited-state nonlinearities are fluence (i.e. energy per unit area) dependent, while the ultrafast effects remain irradiance dependent. The explicit temporal dependences of the nonlinearities can be obtained from, for example, degenerate four-wave mixing experiments [29] or time resolved Z-scan experiments which can separate $\Delta n(t)$ and $\Delta\alpha(t)$ [10,11].

These time-resolved experiments can, in principle, separate slow and fast nonlinear responses. In addition, nondegenerate nonlinearities can be determined from pump-probe[30], four-wave mixing[29] , or 2-color Z-scan [8,9], etc. experiments. These nondegenerate nonlinear responses are also useful in distinguishing various contributing nonlinear mechanisms.

We illustrate the potential problems associated with interpreting nonlinear measurements with a single example of comparing excited-state absorption (reverse saturable absorption) and two-photon absorption signals. The equation describing 2PA in the presence of residual linear absorption is:

$$\frac{dI}{dz'} = -\alpha I - \beta I^2 . \quad (32)$$

Excited states created by linear absorption in molecules are characterized by a $\Delta\alpha \approx \frac{\alpha\sigma}{\hbar\omega}\int_{-\infty}^{t} I(t')dt'$.[15,16] By temporally integrating the resulting equation for dI/dz', we find the fluence F (energy per unit area) varies with z' as [16]

$$\frac{dF}{dz'} = -\alpha F - \frac{\alpha\sigma}{2\hbar\omega}F^2 . \quad (33)$$

Notice that this equation is exactly analogous to the equation describing 2PA loss (Eq. 32) with the fluence replacing the irradiance and $\alpha\sigma/2\hbar\omega$ replacing β. Therefore, since in most experiments the pulse energy is detected, excited-state absorption initiated by linear absorption and 2PA will give nearly identical results for loss as a function of input energy (microscopically ESA can be considered as the limit of 2PA with a resonant intermediate state). The difference between Eqs. 32 and 33 when determining the transmitted energy is in the temporal integral over the pulse for 2PA. For ESA this integral has already been performed. In other words, in order to determine which of these nonlinearities is present, the temporal dependence must be measured in some way. An analogous problem exists with excited-state refraction and the bound electronic n_2. Additionally, as seen in many semiconductors [17] and in some organic materials, [31,32] the excited states can be created by nonlinear absorption (e.g. 2PA) leading to fifth-order nonlinear absorption and refraction, further confusing interpretation.

Equation 33 is only valid for low fluence where the changes in transmittance are small. For higher fluence saturation of the ground state absorption process (or even the excited state absorption [33]) can occur. In such cases the best approach is to solve the system of rate equations to determine the level populations and then use these in the loss equation (Eq. 34) in terms of absorption cross sections, σ_{ij} , or phase equation (Eq. 35) using refractive cross sections $(\sigma_r)_{ij}$:

$$\frac{dI}{dz'} = -\sum_{i=1, j>i}^{N} \sigma_{ij}\Delta N_{ij}\ I \quad (34)$$

$$\frac{d\phi}{dz'} = \sum_{i=1, j>i}^{N} (\sigma_r)_{ij}\Delta N_{ij} \ , (35)$$

where ΔN_{ij} is the population difference between two levels (N_i -N_j) coupled by an absorption cross section σ_{ij} . The nonlinear refractive is due to the redistribution of level populations and the sign depends on the frequency position with respect to the resonance frequency as well as on whether the loss increases or saturates. For many materials (e.g. organic reverse saturable absorbers) ΔN_{ij} can be replaced by the the population of the lower level N_i, since the upper level rapidly decays to an intermediate level (e.g. in the vibration/rotation band).[34] Temporal and spatial integrals of Eqs. 34 and 35 also need to be performed numerically. This procedure, of course, leads to Z-scans where the loss or refraction are not described by the third-order analysis given in this paper. This can also be said of the simple 2-level saturation model which is only described by a third-order response for small fluence.

It is important to note the importance of accurately measuring the laser mode and pulse parameters. For example, 2PA is irradiance dependent. Thus, given the pulse energy, we need to know both the beam area (i.e. spatial beam profile) and the temporal pulsewidth (i.e. temporal shape) in order to determine the irradiance. Any errors in the measurement of irradiance translate to errors in the determination of β as well as several other nonlinear coefficients.

There are several other papers that report methods or analysis for Z-scans that we have not yet mentioned. For example, Herman et. al. discuss factors that affect optical limiting in thin samples with large nonlinearities related to Z-scans in Ref. [35]. In Ref. [36], Hochbaum discusses the simultaneous determination of two or more nonlinear refractive constants in Z-scan measurements. Sutherland describes the effects of multiple internal reflections within a sample on the Z-scan signal in Ref. [37].

For some materials the light permanently or temporarily changes the optical properties so that the sample properties change within the duration of a Z-scan experiment. Oliveira et. al. discuss the analysis of such data.[38] Petrov et.al. describe the use of a Z-scan in a reflection mode to determine changes of the complex dielectric function at surfaces.[39] Kershaw desribes his analysis of EZ-scan measurements in Ref.[40], and a method to enhance the sensitivity of a 2-color Z-scan is described in Ref. [41].

6. Data

The following table gives the results of Z-scan measurements on a variety of organic samples. There is no guarantee of the completeness of the given examples. Reported in Table 1 are values of nonlinear absorption coefficients, n_2's, third-order nonlinear susceptibilities, $\chi^{(3)}$, and hyperpolarizabilities, as defined by the authors in the references cited. Other nonlinear coefficients such as thermal index changes and excited-state cross sections are also given. We also include our own measurements of CS_2 for reference.[42] . We recommend consulting the original literature for numerical values and definitions. In fact, this table is primarily meant to be used a guide to determine which references are of interest to the reader. A brief description of some of the findings from these measurements follows. As can be seen in this literature, the Z-scan technique has been used to measure many different nonlinear mechanisms in organic materials, some identified and some not. Table 2 lists a number of definitions of materials, solvents, techniques etc. used both in Table 1 and in the descriptive text that follows.

6.1 Description of Measurements

Winter et. al. [43], and Oliver et. al. [44] (same study) measured $\chi^{(3)}$ of several nickel dithiolene compounds (metal-sulfur ligand complexes) in a PMMA host with 100 ps pulses at 1064 nm. The SPIE proceedings data supersedes the Opt. Commun. publication.[45] Nonlinear refractive indices, n_2, calculated for neat solutions as high as 10^{-11} cm²/W were found, however, as the concentration increased the $\Delta\alpha$ increased more rapidly than Δn making them less desirable for all-optical switching applications. This was attributed to intermolecular interactions such as dimer and trimer complex formation.

Underhill et. al. [46] used DFWM and Z-scan to study NLA and NLR in PMMA films doped with Ni-dithiolene oligomers at 1064 nm to determine their suitabliltiy for all-optical switching applications. They report favorable figures-of-merit for some of the compounds but no nonlinear coefficients are given.

Gall et.al.[47] incorporate a number of dyes into sol-gels and find that the nonlinear response doesn't change from the solution values using DFWM. They also report Z-scan measurements on CAP in a xerogel with 15 ns 532 nm pulses with w_0= 7 μm, but give no values of the nonlinear coefficients.

The study by Lawrence et. al. [48] reports a large purely refractive nonlinear index, n_2=2.2x10^{-12} cm²/W, of single crystal polydiacetylene paratoluene-sulfonate (PTS) at a wavelength of 1.6 μm. There is no measurable 2PA, and the linear

absorption is ≈1 cm^{-1}, making this material useful for all-optical switching applications. A plot of the effective n_2 versus irradiance shows a straight line with a negative slope indicating that there is a fifth order nonlinearity reducing the total index change at higher irradiance levels.

The same group in Ref. [49] report the measurement of the full 2PA spectrum of PTS from $0.8E_g$ to $1.6E_g$ where E_g is the bandgap energy of PTS. They also report dispersion of n_2 over a smaller wavelength range where the Z-scan signal is not overly dominated by nonlinear absorption. This is the only case known to the authors where the nonlinear absorption and nonlinear refraction of an organic material has been studied over such a large spectral range. Figure 9 shows the spectrum of the two-photon absorption coefficient (Fig. 9a) along with the dispersion of n_2 (Fig. 9b).

In another study, Kim et. al. [50] studied the usefulness of PTS as an all- optical switching material at 1.3 μm. These authors measure n_2 and β at 1.3 μm for 100 ps pulses in a sample of PTS 210 μm thick. They see higher order effects reducing the nonlinear refraction and raising the nonlinear absorption as the input irradiance is increased. However, they find the figures of merit are within the range necessary for all- optical switching. [20]

A similar study of PTS at 1064 nm by Lawrence et. al. [51] measures β and positive n_2, of PTS using 35 ps pulses. Again a fifth-order nonlinear absorption and refraction are observed. The fifth-order nonlinear absorption reduces the loss as the irradiance increases, and the fifth-order nonlinear refraction reduces the index, turning the refraction to self- defocusing above ≈7 GW/cm².

Thakur et. al.[52] measure PTS using Z-scan with 70 ps and 10 ps 1.06 μm pulse trains where the repetition rate and average power are controlled with a Pockels cell. They report a negative $n_2=(-1.5\pm0.5)\times10^{-5}$ cm^2/MW and β=(65±12) cm/GW.

In another series of experiments aimed at measuring the nonlinear spectrum of an organic material, Cha et. al. [53] report β of a di-alkyl-amino-nitro-stilbene side chain polymer, DANS, from 780 to 1600 nm. They find a single 2PA peak at 920nm with a maximum value of β=5.5 cm/GW.

Reference [54] reports measurements of self-focusing at 1064 nm and self-defocusing at 532 nm using 30 ps pulses in a THF solution of phenylmethyl polysilane. They attribute the change in sign at 532 nm to a two-photon absorption resonance transition.

The authors of Ref. [55] measure both β and n_2 of thiophene oligomers for different numbers of repeat units (n=2-6) for 10^{-3} molar solutions in dioxane at 532 nm using 30 ps pulses. They measure self-defocusing which increases in magnitude with chain length. They also find that β increases with chain length.

Measurements of the self-defocusing and nonlinear absorption in polythiophene thin films are reported in Ref. [56]. The nonlinearities at 532 nm using 30 ps pulses are attributed to saturation of the strong linear absorption ($\alpha\approx4\times10^4$ cm^{-1}) at this wavelength.

Samoc et. al.[57] measured a derivative of 1,2-5,6 dibenzoxalene in chloroform (1.2% by weight) using 100 femtosecond pulses at 800 nm using Z-scan to determine a hyperpolarizabiltiy of 1.7×10^{-34} esu which they claim is in reasonable agreement with theoretical predictions.

Measurements of n_2 in Disperse Red 1 are described by Planas et. al.[58] at a wavelength of 1064 nm which is below the 2PA resonance which occurs at 2x490 nm (980 nm) where they find $n_2<0$ ($n_2=-0.8\times10^{-12}$ cm^2/W). Measurements at 1064 nm of n_2 in HITC (1,1',3,3,3',3',-Hexamethylindotricarbocyanine Iodide) where the frequency is above the 2PA resonance at 2x755 nm (1510 nm) give $n_2>0$ ($n_2=3.2\times10^{-12}$ cm^2/W) while β≅30 cm/GW. Both materials were incorporated in thin (several μm thick) PMMA wafers and the laser used produced 100 ps Q-switched pulse trains. These results suggest that the large values of n_2 observed in these materials are associated with a 2PA resonance enhancement

In Ref. [31] measurements were made of the irradiance dependence of the nonlinear response of THF solutions of a bisbenzthiozole-substituted thiophene compound, BBTDOT, and in a didecyloxy substituted polyphenyl compound, DDOS. In both compounds third and fifth order responses were observed for the nonlinear refraction as well as for the nonlinear absorption. The third-order responses are attributed to 2PA and bound electronic refraction while the fifth-order responses are attributed to absorption and refraction from the two-photon generated excited states. Hyperpolarizabilities, n_2, and excited state cross sections for both absorption and refraction are reported. Both compounds show increasing nonlinear absorption with irradiance, i.e., positive fifth-order absorption, while the excited-state refraction is self defocusing in both materials. BBTDOT shows third-order self focusing while DDOS shows third order self defocusing. Reference [59] reviews some of the work contained in Ref. [31] along with several other measurements.

Fleitz et. al.[60] report Z-scan measurements of molten diphenylbutadiene (trans-trans 1,4-diphenyl-1,3-butadiene) at 154°C in a 1 mm cell using 532nm, 35ps pulses. They interpret the increasing nonlinear loss with irradiance as 2PA followed by excited-state absorption.

Reference [61] reports measurements of n_2 of water, salt water and vitreous humor (human and rabbit) at 532 nm using 60 ps pulses. The data show only minor differences between these materials within the measurement errors.

Measurements reported in Ref. [62] of $\chi^{(3)}$ at 532 nm with 20 ns pulses in various concentrations of a series of molybdenum-based metal-organic complexes in solution were made to determine the molecular hyperpolarizability, n_2. A close correlation is reported between the number of delocalized π electrons and the magnitude of n_2.

Reference [63] presents a study of the kinetics of intramolecular proton transfer using picosecond excitation followed by four-wave mixing studies. However, Z-scans of the solvent and solvent plus HBT were made in the nonresonant spectral range to determine the small but positive index change at 1064 and 532 nm.

The authors of Ref. [64] use a cw HeNe laser at 633 nm to measure DFWM and Z-scan signals where they determine $n_2 = 6\text{x}10^{-4}$ esu ($\chi^3 \cong 10^{-4}$ esu) attributed to the slow realignment of the long chain molecules of azobenzene-compound-doped poly(methyl methacrylate) with a push group -NH-$C_{16}H_{23}$ and pull group -NO_2 attached. The sample was in the form of a 0.01 cm thick film.

Song et. al. [65] use continuous wave illumination at 633, 514, 488 and 477 nm of bacteriorhodopsin films to demonstrate self-defocusing index changes of $\approx 10^{-3}$ and anomalous nonlinear absorption.

Song et. al.[66] use the Z-scan at 633 nm and 476 nm (cw) to measure saturation and index changes due to population redistribution (2-level model) and thermal self-defocusing in chemically enhanced bacteriorhodopsin films. For example, they determine saturation intensities of $\cong 3$ mW/cm² at 476nm and $\cong 4$ mW/cm² at 633 nm.

Measurements of a series of inorganic metal cluster molecules are studied and described in Refs. [67,68,69] by S. Shi et. al. Using acetonitrile as the solvent they measure NLA and NLR in the inorganic metal cluster molecules $C_{35}H_{72}N_5OS_6Cu_3Mo$, $WCu_2OS_3(PPh_3)_4$ and $MoCu_2OS_3(PPh_3)_3$.

The same group in Ref. [70] compares the nonlinearities of C_{60} to nonlinearities observed in other inorganic complexes and conclude that the nonlinear response is dominated by nonlinear absorption in both materials.

Gu et. al. [71] measure nonlinear absorption and self-focusing in C_{60} thin films using cw 633 nm light. They attribute the nonlinear absorption to excited triplet state absorption.

In toluene solutions of C_{60}, Mishra et. al. [72] report nonlinear absorption and self-defocusing with 30 ns, 527 nm pulses. They also attribute some loss to nonlinear scattering of a thermal origin.

Justus et. al. [73] attribute the nonlinear absorption they observe in C_{60} in 1-chloronaphthalene using 6 ns 532 nm pulses to excited-state absorption. They attribute the self lensing to photoinduced thermal refractive index changes.

Yang et. al. [74] measure the excited-state absorption cross section of C_{70} as $\sigma = 2.8\text{x}10^{-17}$ cm² using 35 ps 532 nm pulses in a 1 mm cell.

Measurements are reported in Ref. [15] (also see Ref. [75]) of the third-order excited-state nonlinear absorption and refraction in chloro-aluminum phthalocyanine, CAP, solutions in ethanol at 532 nm using 30 ps pulses. Solutions of SiNc, a silicon naphthalocyanine derivative, $Si(OSi(n\text{-hexyl})_3)_2Nc$, in toluene were also studied. By measuring the nonlinearities at two different pulsewidths (30 and 60 ps) they determined that the nonlinearities were both fluence dependent and, thus, due to populating the excited state. They report excited state absorption cross sections, σ, and extinction coefficients. They also give excited state refractive coefficients defined by $d\phi/dz = \sigma_r N$, where ϕ is the induced phase distortion, σ_r the refractive cross section and N the density of excited states. For CAP they report, $\sigma = 2.3\text{x}10^{-17}$ cm² or $\varepsilon = 6\text{x}10^3$ liters $M^{-1}cm^{-1}$, and $\sigma_r = 1.8\text{x}10^{-17}$ cm², while for SiNc, $\sigma = 3.9\text{x}10^{-17}$ cm², $\varepsilon = 1.0\text{x}10^4$ $M^{-1}cm^{-1}$ and $\sigma_r = 4.7\text{x}10^{-17}$ cm².

Wood et. al.[76,77] report Z-scan measurements of excited-state absorption in zinc meso-tetra(p-methoxyphenyl) tetrabenzporphyrin called TBP dissolved in THF using 532 nm, 9 ns pulses. They use a quasi 3-level model to determine $\sigma_{ex} = 2.4\text{x}10^{-16}$ cm² and $\sigma_r = (-0.4 \pm 0.1)\text{x}10^{-16}$ cm², while the ground state cross section is $\sigma_{gr} = 8.0\text{x}10^{-18}$ cm².

Swatton et. al.[78,79,] and Welford et. al. [80] report excited state absorption in HITCI in methanol using 15 ns, 532 nm pulses and describe the observed saturation of the Z-scan signal using a 4-level model which also yields level lifetimes.

The eclipsing Z-scan (EZ-scan) is used in Ref. [7] to measure nonlinear refraction in neat toluene as well as to demonstrate the technique as compared to the Z-scan. The demonstrated sensitivity enhancement is ≈13 under the experimental conditions reported. The nonlinear refraction may have contributions from electrostriction as nanosecond pulses were used.

Xia et. al. [81] report the use of EZ-scan with picosecond pulses to measure nonlinear refraction and nonlinear absorption in thin films. They demonstrate the method by measuring purely nonlinear absorption in a 0.7 μm thick sample of CdSe clusters embedded in CuPC. They speculate that the nonlinearity is dominated by excited-state absorption initiated by linear absorption (RSA). They also report measurements on a 0.5 μm thick BaF_2 film containing ≈30% CuPC showing a combination of NLR and NLA, again probably due to excited-state processes.

The authors of Ref. [82] measure the thermal nonlinearity in a dye doped colloidal crystal using Z-scan and use the distributed feedback structure for power limiting. The limiting is restricted to a narrow spectral bandwidth due to the diffractive nature of the limiting (i.e., Bragg scattering from the nonlinearly induced grating).

Yuan et. al.[83] measure β and n_2 in the pure nematic liquid crystal 5CB (4-cyano-4'-n-pentylbiphenyl) in the isotropic and nematic phase using cw 514 nm light (10 ms shuttered pulses) as a probe with 7 ns 532 nm excitation pulses in a 2-color Z-scan. They find large NLA and NLR for the optical electric field parallel to the director in the nematic phase using 25 μm thick aligned samples. For 7 ns, 532 nm pulses they find β=320 cm/GW and n_2=-1.7x10^{-9} esu (-2.4x10^{-16} m^2/W) for parallel polarizations of the beams (not measurable for perpendicular polarizations). Using 10 ms, 514 nm light they measured n_2 versus temperature for parallel and perpendicular polarizations and find large changes near the critical temperature for $n_2\parallel$ and $n_2\perp$. They observed no NLA for 10 ms pulses.

Optical reorientation measurements in dye doped nematic liquid crystal films are reported in Ref. [84]. The change of the optical path in a nematic film from the light induced director reorientation and from thermally induced refractive index variations are measured separately and the η parameter (ratio of dye induced torque to the normal optical torque) determined. It was found that the dye induced torque significantly exceeds the normal optical torque.

The aperture transmission in a Z-scan measurement is temporally resolved in Ref. [85] to determine the speed of response nonlinear refraction. This method is applied to observe the thermal nonlinearity of methyl nitoanaline.

In two papers, Tian et. al. [86] and [87], attribute the nonlinear refraction observed in Chinese tea in ethyl alcohol to linear absorption induced thermal self-defocusing.

In a similar study Gheung et. al. [88] measure self-defocusing and absorption saturation of tea in water using 532 nm, 7 ns pulses. The index nonlinearity is again attributed to thermal lensing.

The dual beam 2-color Z-scan is used in Ref. [11] to time resolve the thermal index changes due to linear or two-photon absorption in organic dyes. The pump beam was 1.06 μm or 532 nm, 6 ns pulses and the nonlinear response was probed with a cw 633 nm laser. The temporal resolution allowed separation of the fast nonlinear response from the slower thermal index changes in toluene, ethanol and chloroform.

7. Conclusion

There are a variety of methods and techniques for determining the nonlinear optical response, each with its own weaknesses and advantages. In general, it is advisable to use as many complementary techniques as possible over a broad spectral range in order to unambiguously determine the active nonlinearities. Z-scan is one of the simpler experimental methods to employ. Despite the wide range of available methods, it is rare that any single experiment will completely determine the physical processes behind the nonlinear response of a given material. A single measurement of the nonlinear response of a material, at a single wavelength, and a single pulsewidth may give very little information on the material. In general such limited data should not be used to judge the device performance of a material or to compare one material to another.

For someone who wants to measure a nonlinear refractive index, an important question to ask is what is the application for which the phase shift is to be used. For example, if optical limiting with nanosecond pulses is the purpose, so that materials having large nonlinear loss for 10 ns pulses is desirable, the pulsewidth to be used is 10 ns. However, in order to determine the physics behind the nonlinear loss it may be useful to look at this loss using shorter or longer pulses.[89]

Nonlinear absorption and refraction always coexist (although with different spectral properties) as they result from the same physical mechanisms. They are connected via dispersion relations similar to the usual Kramers-Kronig relations that connect linear absorption to the linear index (or, equivalently, relate the real and imaginary parts of the linear susceptibility.[25,26,27,28] The physical processes that give rise to NLA and the accompanying NLR include "ultrafast" bound electronic processes, "excited state" processes where the response times are dictated by the characteristic formation and decay times of the optically induced excited states, thermal refraction, etc. Ultrafast processes include multi-photon absorption[22,23], stimulated Raman scattering [24] and AC-Stark effects [25,26]. Excited-state nonlinearities can be caused by a variety of physical processes including absorption saturation[90], excited-state absorption in atoms or molecules [15] or free-carrier absorption in solids [17,91], photochemical changes[92], as well as defect and color center formation[93]. The above processes can lead to increased transmittance with increasing irradiance (e.g. saturation, Stark effect) or decreased transmittance (eg. multi-photon absorption, excited-state absorption). A key to distinguishing these processes is to pay particular attention to the temporal response. One way of achieving this is the use of pulsewidths much shorter than the decay times of the excited states. In this regime, the excited-state nonlinearities are fluence (i.e. energy per unit area) dependent, while the ultrafast effects remain irradiance dependent.

The Z-scan has only recently been introduced as a useful technique for measuring nonlinearities and there are still relatively few measurements of organic materials using this technique. However, its use as both an absolutely calibrated method for determining standards and as a relative measurement method is increasing. The Z-scan signal as a function of irradiance and/or Z can give useful information on the order of the nonlinearity as well as its sign and magnitude.

8. Acknowledgment

We gratefully acknowledge the support of the National Science Foundation grant ECS#9510046, and the Naval Air Warfare Center Joint Service Agile Program Contract N66269-C-93-0256. The work presented in this paper represents many years of effort involving colleagues and many former and current students as well as post-doctoral fellows. We thank all those involved and acknowledge their contributions through the various referenced publications. We explicitly thank Edesly J. Canto-Said, J. Richard DeSalvo, Arthur Dogariu, David J. Hagan, David C. Hutchings, Ali A. Said, M.J. Soileau, Hermann Vanherzeele, Tai H. Wei, William E. Williams, Brian Wherrett, Milton A.Woodall, Yuen-Yen Wu and Tiejun Xia for their many contributions.

Figure Captions

Figure 1. The Z-scan apparatus used to reduce the noise by monitoring the ratio of detector outputs of Sig. to Ref. (signal to reference). "Open aperture" Z-scans are obtained by removing the apertures (or disks for EZ-scan) shown in front of the signal and reference detectors and carefully collecting all of the transmitted light.

Figure 2. A typical Z-scan for positive (solid line) and negative (dashed line) third-order nonlinear refraction.

Figure 3. A comparison of EZ-scan data and Z-scan data for a self-focusing nonlinearity.

Figure 4. A typical open aperture Z-scan signal for third-order nonlinear absorption.

Figure 5. Calculations of closed and open aperture Z-scan data along with their ratio for self-defocusing accompanied by nonlinear absorption.

Figure 6. Excite-probe Z-scan apparatus. The filter in front of the detector transmits only the probe.

Figure 7. Normalized transmittance for thick samples with L/Z_0 =1,2,5,,8,10 for $\Delta\Phi_{z0}$ =-0.01, as a function of Z/Z_0.

Figure 8. The effective sample length, L_{eff}, in units of n_0Z_0, as a function of L/n_0Z_0.

Figure 9. a) Two-photon absorption coefficient, $\beta = \alpha_2$ (I=0), as a function of two-photon energy in PTS. The inset shows how the 2PA coefficient was determined from the low intensity intercept of the α_2 versus intensity curve. The slope is due to a fifth-order nonlinear absorption process. b) Nonlinear refractive index, n_2, as a function of photon energy for PTS. (from Ref. [49] with permission.)

Table 1
Nonlinear Properties of Organics as Measured by Z-Scan

Material	Solvent	λ (nm)	τ_p (nsec)	L	Beam Radius	2PA Coefficient β (cm/GW)	n_2 (cm^2/W)	Ref.	α (cm^{-1})	Additional information
CS_2	neat liquid	1064 532	0.04 0.028	1 mm 1 mm	25 μm	≈0 ≈0	$3.1(\pm0.2)x10^{-14}$ $3.1(\pm0.2)x10^{-14}$	42 2	≈0 ≈0	reorientational Kerr effect
Ni:dithiolene polymer	PMMA	1064	0.10	5-18μm		13 to 840 at high conc.	$4.2x10^{-10}$ to $1.0x10^{-7}$ at high conc.	43,44	50	NLA increases faster than NLR with conc.
Ni:dithiolene polymer	DCM	1064	0.10	1 mm		0.55	$-1x10^{-14}$	43,44	50	
PTS	single crystal	1600	0.065	210μm	17 μm	<0.5	$2.2(\pm0.3)x10^{-12}$	48	≈1	see higher order NLR & NLA
PTS	single crystal	1610-1120	0.065			up to 200 at 1.05 eV	$(-2 \text{ to } +5)\ x10^{-12}$	49	≈1	spectra given
PTS	single crystal	1064	0.035			100	$+5x10^{-12}$	49	≈1	spectra given
PTS	single crystal	950-800	0.065			up to 700 at 1.35 eV		49	≈1	spectra given
PTS	single crystal	1300	0.20	210μm		20±4	$3.2\pm0.3x10^{-12}$	50	≈1	see higher order NLR & NLA
PTS	single crystal	1064	0.035	210μm	20 μm	100±20	$5(\pm1)x10^{-12}$	51	≈1	see higher order NLR & NLA
PTS	single crystal	1064	0.07 &0.01			65±12	$-1.5(\pm0.5)x10^{-11}$	52		control rep. rate
DANS	50 % by volume in polymer	780-1699	0.003	300μm		up to 5.5 at 920 nm		53		peak 2PA at 920 nm
phenylmethyl polysilane polymer	0.5 M/l THF	532	0.03	1 mm	≈18 μm	0.027	$-2.1x10^{-14}$	54	"≈0"	
phenylmethyl polysilane polymer	0.5 M/l THF	1064	≈0.04	1 mm	≈48 μm	"≈0"	$\approx+1.5x10^{-15}$	54	"≈0"	
thiophene oligomers nT n=2-5	dioxane 10^{-3} m/l	532	0.03	1 mm	26 μm	(1T) 0.026; (4T) 0.11	(1T)+4.9; (3T)-0.5 (4T)-2.3; (5T)-3.2 all $x10^{-15}$	55	"≈0"	sat. of 2PA at 35 GW/cm^2
thiophene oligomers nT n=6	2,5-DCHEX	532	0.03	1 mm	26 μm	(6T) 0.23-0.34	(6T)-3.5 $x10^{-15}$	55	1.4	sat. of 2PA at 35 GW/cm^2
polythiophene	thin film	532	0.03		50 μm	saturation I_{sat}=6.15 GW/cm^2	$-9x10^{-11}$	56	$4x10^4$	NLR from saturation of abs.
Pseudoazulene	chloroform 1.2% weight	800	0.0001	1 mm		$\gamma_r=1.7x10^{-34}$ esu		57		
Disperse red 1	PMMA	1064	0.10 train	few μm		≈0	$-0.8x10^{-12}$	58		2PA enhanced

Material	Solvent	λ (nm)	τ_p (nsec)	L	Beam Radius	2PA Coefficient β (cm/GW)	n_2 (cm^2/W)	Ref.	α (cm^{-1})	Additional information
HITCI	PMMA	1064	0.10 train			30	$3.2x10^{-12}$	58		2PA enhanced

diphenylbutadiene	neat liquid	532	0.035	1 mm	27 μm	2.65	6.3×10^{-12}	60		molten at 154^0C
BBTDOT	0.02M/l THF	532	0.032	0.2 cm	19 μm	$\gamma_I=4.8\times10^{-34}$ esu	$\gamma_r=4.8\times10^{-34}$ esu	31	<0.1	3rd and 5th order
DDOS	5×10^{-3} M/l THF	532	0.032	0.2 cm	19 μm	$\gamma_I=1.1\times10^{-33}$ esu	$\gamma_r=-4.5\times10^{-34}$ esu	31	<0.1	3rd and 5th order
vitreous humor		532	0.060	1 mm	15 μm	$<4\times10^{-3}$	rabbit= $(8.7\pm1.9)\times10^{-16}$ human=$4.5\pm1.3)\times10^{-16}$	61	≈0	
cis-$Mo(CO)_4(PPh_3)_2$	THF	532	20			≈0	$\chi^3=4.6\times10^{-9}$ esu	62	<0.1	derived χ^3
trans-$Mo(CO)_4(PPh_3)_2$	THF	532	20			≈0	$\chi^3=1.4\times10^{-9}$ esu	62	<0.1	derived χ^3
cis-$Mo(CO)_4(PPh_2Ome)_2$	THF	532	20			≈0	$\chi^3=2.6\times10^{-10}$ esu	62	<0.1	derived χ^3
cis-$Mo(CO)_4(PPh_2Me)_2$	THF	532	20			≈0	$\chi^3=1.7\times10^{-10}$ esu	62	<0.1	derived χ^3
$MO(CO)_5(PPh_3)$	THF	532	20			≈0	$\chi^3=8.2\times10^{-11}$ esu	62	<0.1	derived χ^3
$MO(CO)_5(PPh_2NHMe)$	THF	532	20			≈0	$\chi^3=5.0\times10^{-11}$ esu	62	<0.1	derived χ^3
HBT	n-hexane	1064	0.02				2.3×10^{-15} $\chi^3=4.7\times10^{-22}m^2/V^2$	63	≈0	#'s for solvent $n_2>0$ for solute
azobenzene	PMMA	633	cw	100 μm		≈0	6×10^{-4} esu	64		slow realignment
Bacteriorhodopsin	dried film	633	cw	150 μm	50 μm		"-4.0×10^{-6}"	65	≈50	4-10 ms decay
Bacteriorhodopsin	dried film	514	cw	150 μm	32 μm		"-3.6×10^{-6}"	65	≈50	4-10 ms decay
Bacteriorhodopsin	dried film	488	cw	150 μm	31 μm		"-3.5×10^{-6}"	65	≈50	4-10 ms decay
Bacteriorhodopsin	dried film	477	cw	150 μm	30 μm		"-3.5×10^{-6}"	65	≈50	4-10 ms decay
Bacteriorhodopsin	dried film	633 &476	cw			$I_{sat}\cong3$mW/cm^2 at 633 $\cong4$ mW/cm^2 at 476	<0	66		saturation of abs. + thermal defocusing
C_{60}	thin film	633	cw	0.6 μm	48.4 μm	"$(8\pm3)\times10^9$"	"0.16×10^{-9}"	71	1×10^4	2 step absorption thermal focus
C_{60}	toluene	527	30	1.0 cm	80 μm	ESA $\sigma_t\approx3\sigma_g$	"<0"	72	0.17	NL Scattering
C_{60}	1-CloroNapth	532	6	50 μm		ESA	dn/dT	73		ESA+thermal lensing
C_{60}	acetonitrile	532	7	0.1 cm	35 μm	ESA	≈0	70	≈3.6	
C_{70}	toluene	532	0.035	1 mm		$\sigma_I=2.8\times10^{-17}$ cm^2		74		ESA
CAP	10^{-3} M/l toluene	532	0.029 & 0.061	0.2cm	28 μm	$\sigma_I=2.3\times10^{-17}$ cm^2	$\sigma_r=1.8\times10^{-17}$ cm^2	15,75	1.8	ESA and ESR
SINC	10^{-3} M/l toluene	532	0.029 & 0.061	0.2 cm	28 μm	$\sigma_I=3.9\times10^{-17}$ cm^2	$\sigma_r=4.7\times10^{-18}$ cm^2	15,75	1.8	ESA and ESR
TBP	THF	532	9	1 mm	21.4 μm	$\sigma_I=2.4\times10^{-16}$ cm^2	$\sigma_r=(-4\pm1)\times10^{-17}$ cm^2	76,77	2.4	ESA & ESR
HITCI	33.5 μM methanol	532	15	1 mm	14.5 μm	$\sigma_I=(38.4\pm0.4)\times10^{-17}$ cm^2		78,79, 80	0.25	ESA

CuPC	30% in BaF_2 film	532	0.028	0.5 μm	29 μm	"$5x10^{3}$"	"$4.3x10^{-11}$"	81		ESA and ESR but quoted effective β and n_2
10^{-5} M Kiton red with polystyrene spheres	colloid susp in H_2O	514	cw	100 μm	45 μm	"≈0"	"$-1.3x10^{-7}$"	82	3	
5CB	nematic	532	7	25 μm		320	$-2.4x10^{-12}$	83		pol ⏐⏐ to alignment
Anthraquinone dye AQ1, AQ2	nematic host	633	cw	35 μm	30 μm	"≈0"	n_2 not given, torque parameter η quoted	84	AQ2 =142	η=238 AQ2 homeotropic film
Anthraquinone dyes D4, D16, D27	E63	633	cw	35 μm	30 μm	"≈0"	n_2 not given, torque parameter η quoted	84	D4=275 D16 =142 D27 =105	D4: η=-95 D16: η=-19 D27: η=-5 homeotropic film
MNA	chloroform	532	65	1 cm	33 μm	"≈0"	<0	85	0.036	response time measurement
Chinese Tea	ethyl alcohol	633	cw	1 mm	variable	"≈0"	$dn/dt=-3.4x10^{-5}$	86	0.6	thermal defocus
Chinese Tea	ethyl alcohol	633	cw	1 mm	variable	"≈0"	$dn/dt=-3.4x10^{-5}$	87	0.6	thermal defocus
black tea extract	H_2O	532	7	1 cm	44 μm	saturation "-0.84"	$-5.7x10^{-14}$	88	1.4	saturation of abs.+ thermal defocusing
toluene	neat solvent	532	4.7	0.1 cm	22 μm	≈0	$7x10^{-15}$	7	<0.01	demonstration of EZ-scan method
toluene; ethanol and chloroform	neat solvents	1064 or 532 +633 probe	6 at 532 nm 9 at 1064 nm +cw probe	2 mm		1PA & 2PA induced thermal index change on cw probe	dn/dT	11		2-color time resolved Z-scan
diphenylbutadiene or R6G	ethanol, H_2O or toluene	as above	as above	2 mm	60 μm +40μm	1PA & 2PA induced thermal index change on cw probe	dn/dT	11		2-color time resolved Z-scan

Table 2.
Definitions for Table 1

Spot sizes quoted as the half-width at the $1/e^2$ point of the maximum of the irradiance when known.
Pulsewidths quoted as the half-width at half maximum when known.

AQ1 = 1,8-dihydroxy, 4,5-diamino, 2,7-diisobutyl-anthraquinone
AQ2 = 1,8-dihydroxy, 4,5-diamino, 2,7-diisopentyl-anthraquinone
azobenzene = film of azobenzene-compound-doped poly(methyl methacrylate) with push group $-NH-C_{16}H_{23}$ and pull group $-NO_2$
BBTDOT = bisbenethiozole-substituted thiophene
CAP = Chloro-aluminum-phthalocyanine
CloroNapth = chloronaphthalene
CuPC = copper phthalocyanine
D4 = N,N'-(4-methylphenyl)-1,4-diamino-anthraquinone in E63
D16 = N-(4-nonyloxylphenyl)-1-amino-4-hydroxy-anthraquinone in E63
D27 = N-(4-dimethylaminophenyl)-1-amino-4-hydroxy-anthraquinone in E63
DANS = a di-alkyl-amino-nitro-stilbene side chain polymer
DCHEX = didecylhexathiophene
DCM = 4-(Dicyanomethylene)-2-methyl-6-(4-dimethylaminostyryl)-4H-pyran
DDOS = Didecyloxy substituted polyphenyl
derived χ^3 = is derived by extrapolating dilute data to the neat material
diphenylbutadiene = trans-trans 1,4-diphenyl-1,3-butadiene
ESA = excited state absorption
ESR = excited state refraction
E63 = a mixture composed mainly of biphenyls developed by British Drug House
few = a few or several
HBT = 2-(2'-hydroxyphenyl)benzothiazole
HITCI = 1,1',3,3',3',-hexamethylindocarbocyanine iodide
nematic = nematic liquid crystal
Ni:dithiolene polymer = modified bis[1-ethyl-2-phenylethene-1,2-dithiolate(2-)-S,S' nickel in PMMA
NLA = nonlinear absorption
NLR = nonolinear refraction
MNA = methyl nitroanaline
PC = phthalocyanine
PMMA = poly-methyl methacrylate
pol = polarization
Pseudoazulene = 1,2-5,6 dibenzoxalene
PTS = poly[2,4-hexdiyne-1,6-diol-bis-p-toluene-sulfonate]
Rep. Rate = repetition rate
sat = saturation
SINC = silicon naphthalocyanine
TBP = zinc meso-tetra(p-methoxyphenyl) tetrabenzporphyrin
THF = tetrahydrofuran
2PA = two-photon absorption
5CB = 4-cyano-4'-n-pentylbiphenyl
$\gamma = \chi^3 \ 3^4/[(n^2+2)^4 N]$, where N is molecular density, n the linear index and γ is in units of $cm^5/statvolt^2$.
σ = excited state absorption cross section defined from $dI/dz = -\sigma NI$ where N is the density of excited states
σ_g = ground state absorption cross section defined from $dI/dz = -\sigma_g NI$ where N is the density in the ground state
σ_r = excited state refractive cross section defined from $d\phi/dz = \sigma_r N$ where N is the density of excited states and ϕ is the field phase
σ_t = triplet state absorption cross section defined from $dI/dz = -\sigma_t NI$

where N is the density of triplet states

Some figures are missing.

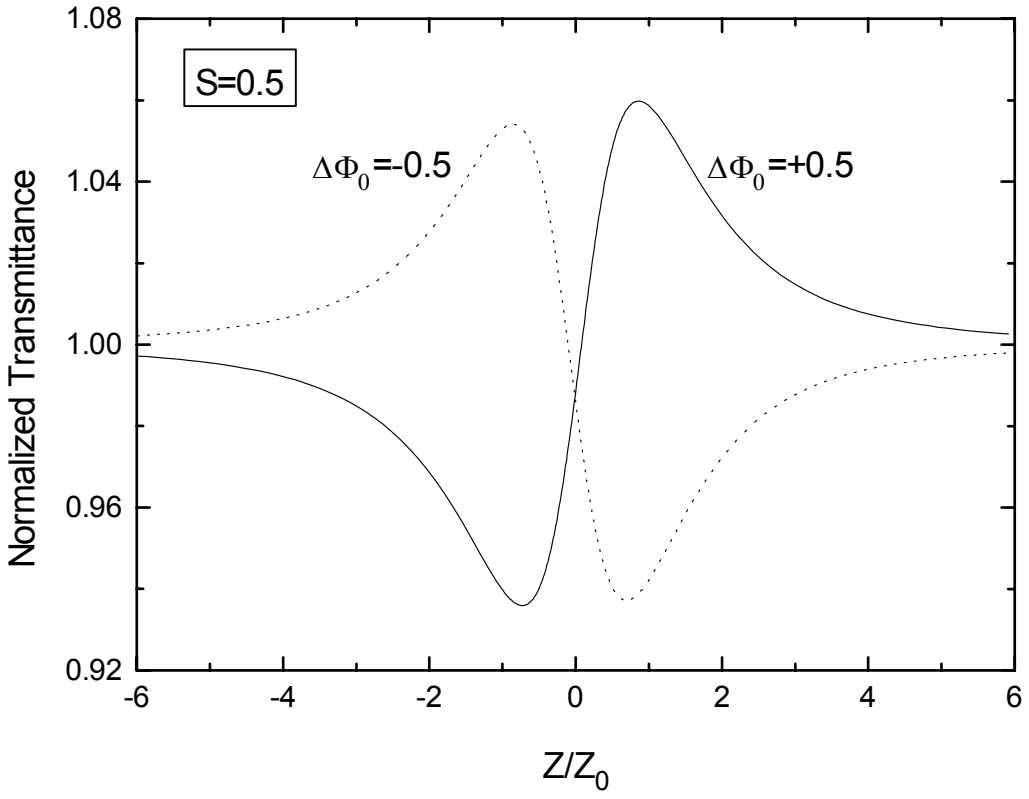

Figure 2. A typical Z-scan for positive (solid line) and negative (dashed line) third-order nonlinear refraction.

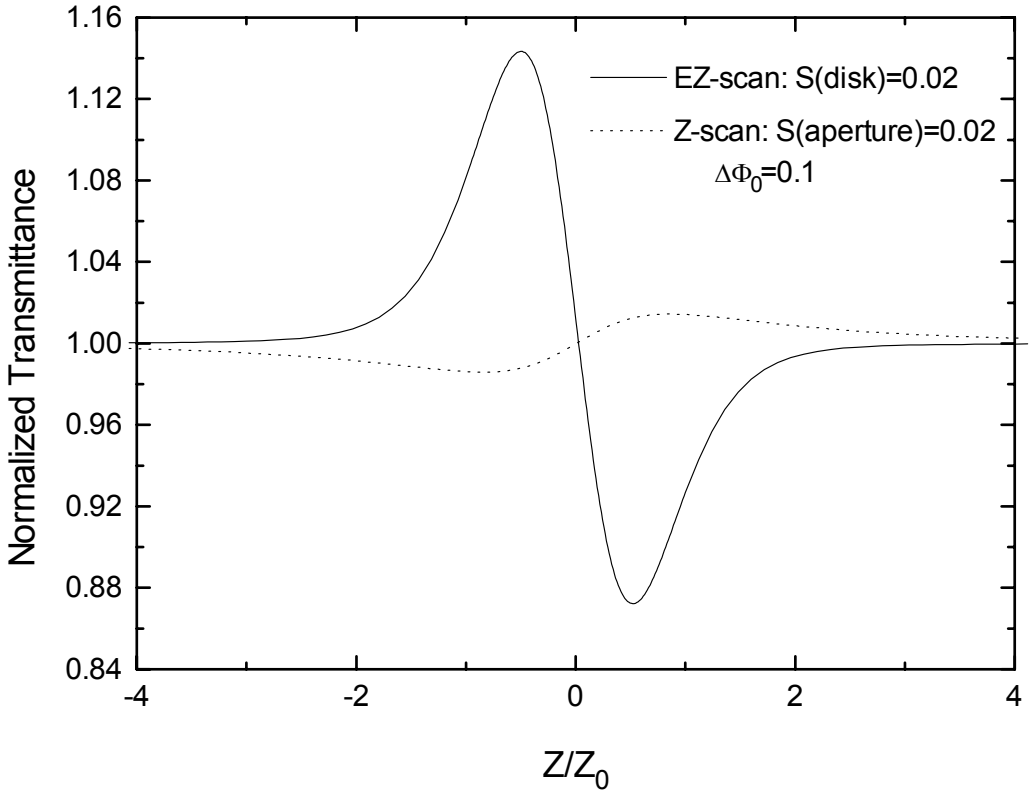

Figure 3. A comparison of EZ-scan data and Z-scan data for a self-focusing nonlinearity

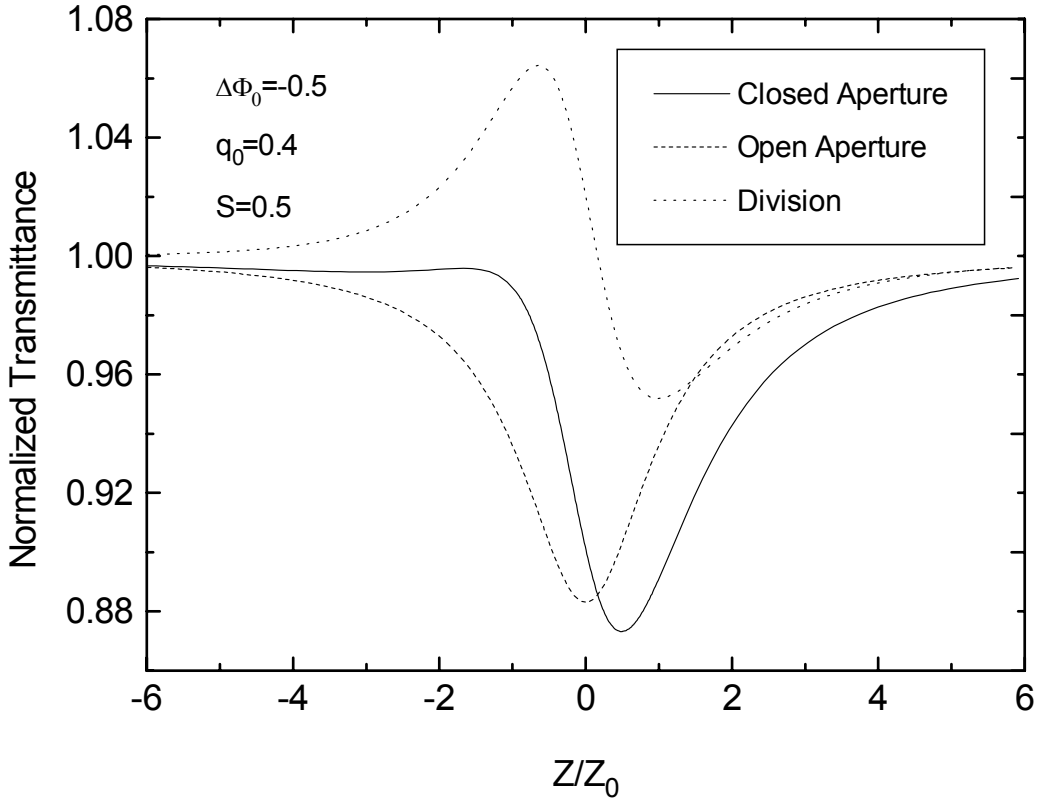

Figure 5. Calculations of closed and open aperture Z-scan data along with their ratio for self-defocusing accompanied by nonlinear absorption.

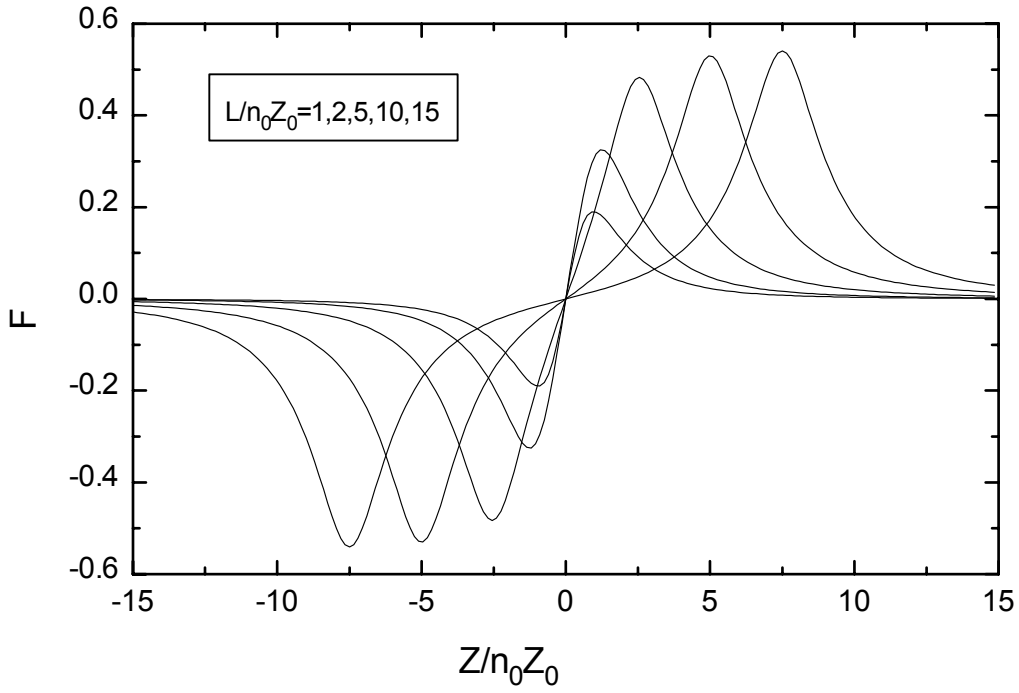

Figure 7. Normalized transmittance for thick samples with L/Z_0 =1,2,5,,8,10 for $\Delta\Phi_{z0}$ =-0.01, as a function of Z/Z_0.

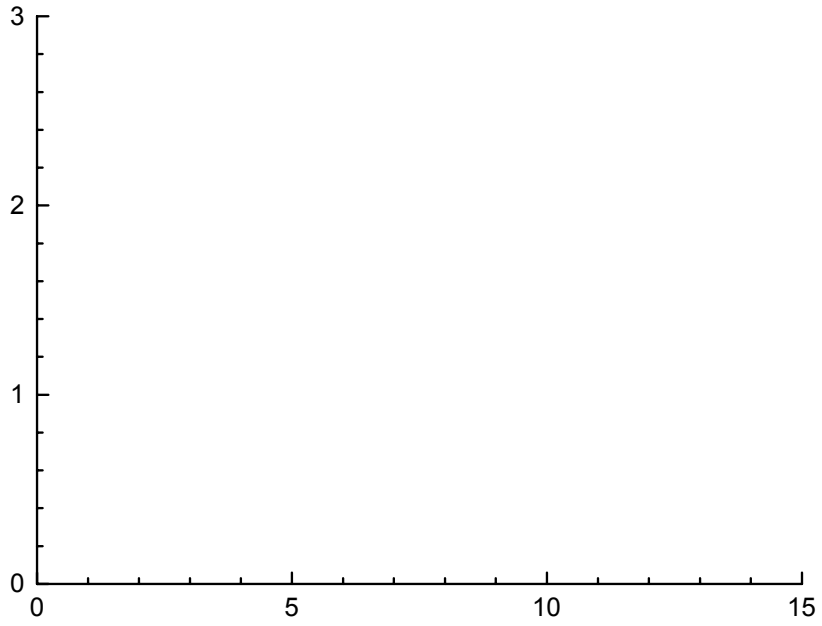

Figure 8. The effective sample length, L_{eff}, in units of n_0Z_0, as a function of L/n_0Z_0.

[1] M. Sheik-Bahae, A.A. Said, and E.W. Van Stryland, "High Sensitivity, Single Beam n_2 Measurements", Opt. Lett. 14, 955-957 (1989).

[2] M. Sheik-Bahae, A.A. Said, T.H. Wei, D.J. Hagan, and E.W. Van Stryland, "Sensitive Measurement of Optical Nonlinearities Using a Single Beam", Journal of Quantum Electronics, JQE QE-26, 760-769 (1990).

[3] M. Sheik-Bahae, A.A. Said, D.J. Hagan, M.J. Soileau, and E.W. Van Stryland, "Nonlinear Refraction and Optical Limiting in "Thick" Media",Opt. Eng. 30, 1228-1235 (1990).

[4] J.A. Hermann and R.G. McDuff, "Analysis of spatial scanning with thick optically nonlinear media", J. Opt. Soc. Am. B10, 2056-2064 (1993).

[5] J.-G. Tian, W.-P. Zang, C.-Z. Zhang, and G. Zhang, "Analysis of beam propagation in thick nonlinear media", Appl. Opt., 34, 4331-4336 (1995).

[6] P.B. Chapple, J. Staromlynska and R.G. McDuff, "Z-scan studies in the thin- and the thick-sample limits", J. Opt. Soc. Am B. 11, 975-982 (1994).

[7] T. Xia, D.J. Hagan, M. Sheik-Bahae, and E.W. Van Stryland, "Eclipsing Z- Scan Measurement of $\lambda/10^4$ Wavefront Distortion", Opt. Lett. 19, 317-319 (1994).

[8] M. Sheik-Bahae, J. Wang, J.R. DeSalvo, D.J. Hagan and E.W. Van Stryland, "Measurement of Nondegenerate Nonlinearities using a 2-Color Z-Scan", Opt. Lett., 17, 258-260 (1992).

[9] H. Ma, A. S. Gomez and Cid B. de Araujo, "Measurement of nondegenerate optical nonlinearity using a two-color single beam method," Appl. Phys. Lett. , Vol. 59, 2666, 1991.

[10] J. Wang, M. Sheik-Bahae, A.A. Said, D.J. Hagan, and E.W. Van Stryland, "Time-Resolved Z-Scan Measurements of Optical Nonlinearities", JOSA B11, 1009-1017 (1994).

[11] V.P. Kozich, A. Marcano, F. Hernandez and J. Castillo, "Dual-beam time-resolved Z-scan in liquids to study heating due to linear and nonlinear light absorption", Applied Spectroscopy 48, 1506-1512 (1994). See also, J. Castillo, V. Kozich and A. Marcano, "Thermal lensing resulting from one- and two-photon absorption studied with a two-color time-resolved Z-scan", Opt. Lett. 19, 171-173 (1994).

[12] W. Zhao and P. Palffy-Muhoray, "Z-scan measurements of χ^3 using top-hat beams", Appl. Phys. Lett., 65, 673-675 (1994). See also, W. Zhao, J. H. Kim and P. Palffy-Muhoray, "Z-scan measurements on liquid crystals using top-hat beams", Appl. Phys. Lett., 65, 673-675 (1994).

[13] A.E. Kaplan, "External Self-Focusing of Light by a Nonlinear Layer", Radiophys. Quant. Electron., 12, 692-696 (1969).

[14] C.R. Giuliano and L. D. Hess, "Nonlninear Absorption of Light: Optical Saturation of Electronic Transitions in Organic Molecules with High Intensity Laser Radiation", IEEE J. Quant. Electron. QE-3, 338-367 (1967).

[15] T.H. Wei, D.J. Hagan, M.J. Sence, E.W. Van Stryland, J.W. Perry, and D.R. Coulter, "Direct Measurements of Nonlinear Absorption and Refraction in Solutions of Phthalocyanines", Applied Physics, B54, 46-51 (1992).

[16] E. Van Stryland, M. Sheik-Bahae, A.A. Said, and D. J. Hagan, "Characterization of Nonlinear Optical Absorption and Refraction", Prog. Crystal Growth and Charact., 27, 279-311 (1993).

[17] A.A. Said, M. Sheik-Bahae, D.J. Hagan, T.H. Wei, J. Wang, J. Young and E.W. Van Stryland, Determination of Bound and Free-Carrier Nonlinearities in ZnSe, GaAs, CdTe, and ZnTe", JOSA B, 9, 405-414 (1992).

[18] R. Bridges, G. Fischer, R. Boyd, "Z-scan measurement technique for non-Gaussian beams and arbitrary sample thicknesses", Opt. Lett., 20, 1821-1823 (1995).

[19] D. Weaire, B. S. Wherrett, D.A.B. Miller, and S.D. Smith, "Effect of Low Power Nonlinear Refraction on Laser Beam Propagation in InSb", Opt. Lett., 4, 331-333 (1974).

[20] V. Mizrahi, K. DeLong, G. Stegeman, M. Saifi and M. Andrejco, “Two-photon absorption as a limitation to all-optical switching”, Opt. Lett. 14, 1140-1142 (1989). See also K. DeLong, K. Rochford and G. Stegeman, "Effect of two-photon absorption on all-optical waveguide devices", Appl. Phys. Lett., 55, 1823-1825 (1989).

[21] P. Banerjee, R. Misra, M. Maghraoui, “Theoretical and Experimental Studies of Propagation of Beams Through a Finite Sample of a Cubically Nonlinear Material”, J. Opt. Soc. Am. B, 8, 1072 (1991).

[22] Bechtel, J. H. and Smith, W. L., “Two-Photon Absorption in Semiconductors with Picosecond Laser Pulses”, Phys. Rev. B, 13, 3515, (1976).

[23] E. W. Van Stryland, H. Vanherzeele, M. A. Woodall, M. J. Soileau, A. L. Smirl, S. Guha, and T. F. Boggess, “Two photon absorption, nonlinear refraction, and optical limiting in semiconductors”, Opt. Eng., 24, 613 (1985).

[24] see for example, Y.R. Shen, The Principles of Nonlinear Optics, John Wiley and Sons, New York, 1984.

[25] M. Sheik-bahae, D.J. Hagan, and E.W. Van Stryland, "Dispersion and Band-Gap Scaling of the Electronic Kerr Effect in Solids Associated with Two-Photon Absorption", Phys. Rev. Lett., 65, 96-99 (1989).

[26] M. Sheik-Bahae, D.C. Hutchings, D.J. Hagan, and E.W. Van Stryland, "Dispersion of Bound Electronic Nonlinear Refraction in Solids", JQE, QE-27, 1296-1309 (1991).

[27] D.C. Hutchings, M. Sheik-Bahae, D.J. Hagan, and E.W. Van Stryland, "Kramers-Kronig Relations in Nonlinear Optics", Optical and Quantum Electronics, 24, 1-30 (1992).

[28] F. Bassani and S. Scandolo, "Dispersion Relations in Nonlinear Optics", Phys. Rev., B44, 8446-8453 (1991).

[29] E.J. Canto-Said, D.J. Hagan, J. Young, and E.W. Van Stryland, “Degenerate Four-Wave Mixing Measurements of High Order Nonlinearities in Semiconductors", JQE, QE-27, 2274-2280 (1991).

[30] D. Von der Linde, A. Laubereau and W. Kaiser, “Molecular vibrations in liquids: direct measurement of the dephasing time; determination of the shape of picosecond light pulses”, Phys. Rev. Lett., 26, 954 (1971).

[31] A.A. Said, C. Wamsley, D.J. Hagan, E.W. Van Stryland, B.A. Reinhardt, P. Roderer, and A.G. Dillard, “Third and Fifth Order Optical Nonlinearities in Organic Materials”, Chem. Phys. Lett., 228, 646-650 (1994).

[32] B.L. Lawrence, M. Cha, W.E. Torruellas, G.I. Stegeman, S. Etemad and G. Baker, “Z-scan Measurement of Third and Fifth Order Nonlinearities in Single Crystal PTS at 1064 nm”, Nonlinear Optics, 10, 193-205 (1995).

[33] T.-H. Wei, T.-H. Huang, H.-D. Lin and S.-H. Lin, “Lifetime Determination for High-Lying Excited States Using Z-scan”, Appl. Phys. Lett. 67, 2266 (1995).

[34] T. Xia, D. Hagan, A. Dogariu, A. Said and E. Van Stryland, “Optimization of Optical Limiting Devices Based on Excited State Absorption”, to be published in Applied Optics (1996).?

[35] J. Hermann and P. Wilson, “Factors affecting optical limiting and scanning with thin nonlinear samples”,Int. J. of Nonlinear opt. Phys., 2, 613-629 (1993).

[36] A. Hochbaum, “Simultaneous determination of two or more nonlinear refractive constants by Z-scan measurement”, Opt. Lett., 20, 2261-2263 (1995).

[37] R. L. Sutherland, “Effects of multiple internal sample reflections on nonlinear refractive Z-scan measurements”, Appl. Opt., 33, 5576-5584 (1994).

[38] L.C. Oliveira and S.C. Zilio, "Single-beam time-resolved Z-scan measurements of slow absorbers", Appl. Phys. Lett., 65, 2121-2123 (1994).

[39] D.V. Petrov, A.S.L. Gomes, Cid B. de Araujo, "Reflection Z-scan technique for measurement of optical properties of surfaces", Appl. Phys. Lett., 65, 1067-1069 (1994).

[40] S.V. Kershaw, "Analysis of the EZ-scan measurement technique", J. Mod. Opt. 42, 1361-1366 (1995).

[41] H. Ma, and C.B. de Araujo, "Two-color Z-scan technique with enhanced sensitivity", Appl. Phys. Lett. 66, 1581-1583 (1995).

[42] present paper, See Table 1.

[43] C. Winter, R. Manning, S. Oliver, and C. Hill, "Measurement of the large optical nonlinearity of nickel dithiolene doped polymers", Opt. Commun. 90, 139-143 (1992).

[44] S.N. Oliver, C.S. Winter, R.J. Manning, J.D. Rush, C. Hill and A.E. Underhill, "Nickel Dithiolene-PMMA guest-host polymers for all optical signal switching", Proc. SPIE, 1775, Nonlinear Optical Properties of Organic Materials V, 110-120 (1992).

[45] R. Manning, private communication

[46] A. Underhill, C Hill, A. Charlton, S. Oliver, and S. Kershaw, "Third-order NLO properties of PMMA films co-dispersed with metal dithiolene oligomers", Synthetic Metals, 71, 1703-1704 (1995).

[47] G. Gall, T. King. S. Oliver, C. Capozzi, A. Seldon, C. Hill and A. Underhill, "Third-order optical properties of metal dithiolene and phthalocyanine doped sol-gel materials", SPIE vol. 2288, Sol-Gel Optics, 372-381 (1994).

[48] B. Lawrence, M. Cha, J. Kang, W. Torruellas, G. Stegeman, G. Baker, J. Meth, and S. Etemad, "Large purely refractive nonlinear index of single crystal P-toluene sulphonate (PTS) at 1600 nm", Electron. Lett. 30, 447-448 (1994).

[49] B. Lawrence, W. Torruellas, M. Cha, M. Sundheimer, G. Stegeman, J. Meth, S. Etemad and G. Baker, "Identification of the role of two-photon excited states in a π-conjugated polymer", Phys. Rev. Lett. 73, 597-600 (1994).

[50] D.Y. Kim, B. Lawrence, W. Torruellas, G. Stegeman, G. Baker, and J. Meth, "Assessment of single crystal p-toluene sulfonate as an all-optical switching material at 1.3 μm", Appl. Phys. Lett. 65, 1742-1744 (1994).

[51] B. Lawrence, M. Cha, W. Torruellas, and G. Stegeman, "Measurement of the complex nonlinear refractive index of single crystal p-toluene sulfonate at 1064 nm", Appl. Phys. Lett. 64, 2773-2775 (1994).

[52] M. Thakur and R. Quintero-Torres, "The sign and magnitude of the off-resonant nonlinearities of Polydiacetylene crystal measured by Z-scan", SPIE vol. 2025, 446-449 (1993).

[53] M. Cha, W. Torruellas, G. Stegeman, W. Horsthuis, G. Mohlmann and J. Meth, "Two-photon absorption of di-alkyl-amino-nitro-stilbene side chain polymer", Appl. Phys. Lett. 65, 2648-2650 (1994).

[54] L. Yang, R. Dorsinville, R. Alfano, W. Zou and N. Yang, "Sign of $\chi^{(3)}$ in polysilane polymers", Opt. Lett. 16, 758-760 (1991).

[55] J. Hein, H. Bergner, M. Lenzner and S. Rentsch, "Determination of real and imaginary part of $\chi^{(3)}$ of thiophene oligomers using the Z-scan technique", Chemical Physics 179, 543-548 (1994).

[56] L. Yang, R. Dorsinville, Q. Wang, P. Ye., R. Alfano, "Excited-state nonlinearity in polythiophene thin films investigated by the Z-scan technique, Opt. Lett. 17, 323-325 (1992).

[57] M. Samoc, J. Swiatkiewicz, A. Samoc, B. Luther-Davies, "Third-order nonlinear optical properties of pseudoazulenes", Acta Physica Polonica A, 88, 411-416 (1995).

[58] S. Planas, A. Duarte, C. Mazzali, E. Palange, H. Fragnito, V. Cardosa, M. sanches, M. Vallani, A. Reggiani, "Nonlinear refractive index of dye-doped organic polymers", SPIE vol. 2025, 381-387 (1993).

[59] E.W. Van Stryland, M. Sheik-Bahae and D.J. Hagan, "Characterization and Modeling of Nonlinear Optical Absorption and Refraction", in Research Trends in Nonlinear and Quantum Optics, American Institute of Physics, Research Trends in Physics Series, to be published? (1996).

[60] P. Fleitz, R. Sutherland and T. Bunning, "Z-scan measurements on molten diphenylbutadiene in the isotropic liquid state", Mat. Res. Soc. symposium proceedings, Vol. 374, , pp. 211-216, eds. R. Crane, K. Lewis, E. Van Stryland and M. Koshnevisan, MRS, Pittsburg (1995).

[61] B. Rockwell, W. Roach, M. Rogers, M. Mayo, C. Toth, C. Cain and G. Noojin, "Nonlinear refraction in vitreous humor", Opt. Lett. 18, 1792-1794 (1993).

[62] T. Zhai, C. Lawson, G. Burgess, M. Lewis, D. Gale and G. Gray, "Nonlinear-optical studies of molybdenum metal organics", Opt. Lett. 19, 871-873 (1994).

[63] T. Hofer, P. Kruck, T. Elsaesser and W. Kaiser, "Transient states of an intramolecular proton transfer cycle studied by degenerate four-wave mixing", J. Phys. Chem. 99, 4380-4385 (1995).

[64] H. Fei, Z. Wei, Q. Yang, Y. Che, Y. Shen, X. Fu and L. Qui, "Low-power phase conjugation in push-pull azobenzene compounds", Opt. Lett., 20, 1518-1520 (1995).

[65] Q. Song, C. Zhang, R. Gross, and R. Birge, "Optical limiting by chemically enhanced bacteriorhodopsin films", Opt. Lett. 18, 775-777 (1993).

[66] Q. Song, C. Zhang, R. Gross, and R. Birge, "The intensity-dependent refractive index of chemically enhanced bacteriorhodopsin", Opt. Commun., 112, 297-301 (1994).

[67] [G] S. Shi, W. Ji, W. Xie, T.C. Chong, H.C. Zeng, J.P. Lang and X.Q. Xin, "The mixed metal cluster $(n\text{-}Bu_4N)_2[MoCu_3OS_3(NCS)_3]$: the first example of a nest-shaped compound with large third-order polarizability and optical limiting effect", Materials Chemistry and Physics, 39, 298-303 (1995).

[68] S. Shi, W. Ji and X.Q. Xin, "Synthesis and superior third-order nonlinear optical properties of the cluster $(n\text{-}Bu_4N)_4[Mo_8Cu_{12}O_8S_{24}]$" J. Phys. Chem., 99, 894-898 (1995).

[69] S. Shi, H.W. Hou, and X.Q. Xin, "Solid state synthesis and self-focusing and nonlinear absorptive properties of two butterfly-shaped clusters $WCu_2OS_3(PPh_3)_4$ and $MoCu_2OS_3(PPh_3)_3$", J. Phys. Chem. 99, 4050-4053 (1995).

[70] S. Shi, W. Ji, J.P. Lang and X.Q. Xin, "New nonlinear optical chromophore: Synthesis, structures, and optical limiting effect of transition-metal clusters $(n\text{-}Bu_4N)_3[WM_3Br_4S_4]$ (W= Cu and Ag)", J. Phys.Chem., 98, 3570-3572 (1994). see also, S. Shi, W. Ji, and S.H. Tang, "Synthesis and optical limiting capability of cubane-like mixed metal clusters $(n\text{-}Bu_4N)_3[MoAg_3\ BrX_3S_4]$ (X = Cl and I)", J. Am. Chem Soc., 116, 3615-3616 (1994).

[71] G. Gu, W. Zhang, H. Zen, Y. Du, Y. Han, W. Zhang, F. Dong, Y. Xia, "Large nonlinear absorption in C_{60} thin films", J. Phys. B: At. Mil. Opt. Phys. 26, L451-L455 (1993).

[72] S.R. Mishra, H.S. Rawat, M.P. Joshi and S.C. Mehendale, "The role of nonlinear scattering in optical limiting in C_{60} solutions", J. Phys. B: At. Mil. Opt. Phys. 27, L157-L163 (1994).

[73] B. Justus, Z. Kafafi, and A. Huston, "Excited-state absorption-enhanced thermal optical limiting in C_{60}", Opt. Lett. 18, 1603-1605 (1993).

[74] L. Yang, E. Royer, A. Walser and R. Dorsinville, "Nonlinear optical responses of C_{70}-toluene solutions", Chem. Phys. Lett. 239, 390-4-3 (1995).

[75] J.W. Perry, L.R. Khundkar, D.R. Coulter, T.H. Wei, E.W. Van Stryland and D.J. Hagan, "Excited State Absorption and Optical Limiting in Solutions of Metallophthalocyanines", proceedings of the NATO workshop on "Organic Materials for Nonlinear Optics and Photonics", La Rochelle, France, Aug. 26-31, 1990.

[76] G. Wood, M. Miller and A. Mott, "Investigation of tetrabenzporphrin by the Z-scan technique", Opt. Lett., 20,973-975 (1995).

[77] G. Wood, A. Mott and M. Miller, "Nonlinear optical properties of Tetrabenzporphyrin", Mat. Res. Soc. symposium proceedings, Vol. 374, , pp. 267-273, eds. R. Crane, K. Lewis, E. Van Stryland and M. Koshnevisan, MRS, Pittsburg (1995).

[78] S.N.R. Swatton, K. Welford, S. Till, and J. Sambles, " Nonlinear absorption of a carbocyanine dye 1,1',3,3,3',3'-hexamethylindotricarbocyanine iodide using a Z-scan technique", Appl. Phys. Lett. 66, 1868-1870 (1995).

[79] S. Swatton, K. Welford, S. C. Ray and S. Till, "Wavelength dependence of the non-linear transmission of HITCI using the z-scan technique", Mat. Res. Soc. symposium proceedings, Vol. 374, pp. 173-177, eds. R. Crane, K. Lewis, E. Van Stryland and M. Koshnevisan, MRS, Pittsburg (1995).

[80] K. Welford, S. Swatton, S. Hughes, S. Till, G. Spruce, R. Hollins and B.S. Wherrett, "Nonlinear absorption in organic dyes", Mat. Res. Soc. symposium proceedings, Vol. 374, pp. 239-256, eds. R. Crane, K. Lewis, E. Van Stryland and M. Koshnevisan, MRS, Pittsburg (1995).

[81] E.W. Van Stryland, M. Sheik-Bahae, T. Xia, C. Wamsley, Z. Wang, A.A. Said, and D.J. Hagan, "Z-scan and EZ-scan Measurements of Optical Nonlinearities", International Journal of Nonlinear Optical Physics, Novel Nonlinear Optical Polymers and Organic Materials, IJNOP, Vol. **3**, 489-500 (1994).

[82] C. Herbert, W. Capinski, and M. Malcuit, "Optical power limiting with nonlinear periodic structures", Opt. Lett. 17, 1037-1039 (1992).

[83] H.J. Yuan, L. Li and P. Palffy-Muhoray, "Nonlinear birefringence of nematic liquid crystals", SPIE vol. 1307, Electro-Optical Materials for Switches, Coatings, Sensor Optics and Detectors, 363-373 (1990).

[84] I. Janossy and T. Kosa, "Influence of anthraquinone dyes on optical reorientation of nematic liquid crystals", Opt. Lett. 17, 1183-1185 (1992). See also, D. Paparo, P. Maddalena, G. Abbate, E. Santamato, and I. Janossy, "Wavelength Dependence of Optical Reorientation in Dye-Doped Nematics", Mol. Cryst. Liq. Cryst., 251, 73-84 (1994).

[85] H. Toda and C. Verber, "Simple technique to reveal a slow nonlinear mechanism in a Z-scan like n_2 measurement", Opt. Lett. 17, 1379-1381 (1992).

[86] J.-G. Tian, C. Zhang, G. Zhang, "The origin of optical nonlinearities of Chinese tea", Optik, 90, 1-4 (1992).

[87] J.-G. Tian, C. Zhang, G. Zhang and J. Li, "Position dispersion and optical limiting resulting from thermally induced nonlineaities in Chinese tea liquid", Appl. Opt. 32, 6628-6632 (1993).

[88] Y. Cheung, and S. Gayen, "Optical nonlinearities of tea studied by Z-scan and four-wave mixing techniques, J. Opt. Soc. Am. B11, 636-643 (1994).

[89] E.W. Van Stryland, "Application of Nonlinear Optics to Passive Optical Limiting", in Nonlinear Optics of Organic Molecular and Polymeric Materials , ed. H.S. Nalwa and S. Miyata, ?, (1995).

[90] See for example, Y.R. Shen, "The principles of nonlinear optics", John Wiley and Sons, New York, 1984.

[91] T.F. Boggess, S.C. Moss, I.W. Boyd, and A.L. Smirl, "Nonlinear optical energy regulation by nonlinear refraction and absorption in silicon", Opt. Lett. 9, 291-293, (1984).

[92] See for example, Kosar in "Light sensitive systems", J. Wiley and Sons, New York, 1965. See also, D.R. Bosomworth and H.J. Gerritson, "Thick holograms in photochromic materials", Appl. Opt., 7, 95 (1968).

[93] Nastaran Mansour, K. Mansour, E. Van Stryland, and M.J. Soileau, "Diffusion of color centers generated by two-photon absorption at 532 nm in cubic zirconia", Journal of Applied Physics, 67, 1475-1477 (1989).